

Robert L. Ehrlich, Jr., *Governor*
Michael S. Steele, *Lt. Governor*



Robert L. Flanagan, *Secretary*
Neil J. Pedersen, *Administrator*

STATE HIGHWAY ADMINISTRATION

RESEARCH REPORT

ESTIMATION OF LONG-TERM SCOUR AT MARYLAND BRIDGES USING EFA/SRICOS

UNIVERSITY OF MARYLAND, COLLEGE PARK

**Project SP107B4E
FINAL REPORT**

December 2004

The contents of this report reflect the views of the authors, who are responsible for the facts and the accuracy of the data presented herein. The contents do not necessarily reflect the official views or policies of the Maryland State Highway Administration. This report does not constitute a standard, specification, or regulation.

Technical Report Documentation Page

1. Report No. MD-04-SP107B4E	2. Government Accession No.	3. Recipient's Catalog No.	
ESTIMATION OF LONG-TERM SCOUR AT MARYLAND BRIDGES USING EFA/SRICOS		5. Report Date December 2004	
		6. Performing Organization Code	
7. Authors K.L. Brubaker, V. Ghelardi, D. Goodings, L. Guy, P. Pathak		8. Performing Organization Report No.	
9. Performing Organization Name and Address Department of Civil & Environmental Engineering 1173 Glenn L. Martin Hall University of Maryland, College Park 20742		10. Work Unit No. (TRAIS)	
		11. Contract or Grant No. SP107B4E	
12. Sponsoring Organization Name and Address Maryland State Highway Administration Office of Policy & Research 707 North Calvert Street Baltimore MD 21202		13. Type of Report and Period Covered Final Report	
		14. Sponsoring Agency Code	
15. Supplementary Notes			
16. Abstract Current design methods to estimate bridge pier scour assume that the soil is non-cohesive (sand, gravel, or cobbles), and thus may overestimate scour at piers that are placed in cohesive soil (clay). Estimates based on assuming non-cohesive soil may be overly conservative, possibly resulting in unrealistically high scour depths and unnecessary costs. This study evaluates a set of hardware and software tools that have been developed to estimate bridge pier scour in cohesive soils: the Erosion Function Apparatus (EFA) and the Scour Rate In Cohesive Soils (SRICOS) method. The state of Maryland is participating in a large-scale evaluation of the methods for soils and bridge crossings in other regions of the U.S. beyond the state of Texas, where they were developed. Five bridge crossing sites in Maryland were identified for analysis. Soil cores (Shelby tube samples) were collected at the sites and analyzed using the Erosion Function Apparatus, a device that physically measures the rates of erosion of the soil. Time series of daily stream discharges were synthesized using a probabilistic method developed in this study to represent the statistical patterns of streamflow for locations where gage data are not available. The SRICOS program takes as input the soil properties determined from the EFA and the synthetic hydrographs to predict the time evolution of scour at bridge piers. The SRICOS scour depth predictions were lower than predicted by the FHWA HEC-18 method, which is currently used in most scour studies, which assumes non-cohesive soil, and which is based on ultimate-development instantaneous peak discharge. EFA/SRICOS has been shown to be applicable to Maryland sites and soils. The method represents a move forward in developing and applying physical tests of soils, and in incorporating that information in prediction techniques that are meaningful and relevant for bridge design.			
17. Key Words Erosion Function Apparatus, EFA, SRICOS, erosion, pier scour, scour, scour rate, cohesive soils		18. Distribution Statement: No restrictions This document is available from the Research Division upon request.	
19. Security Classification (of this report) None	20. Security Classification (of this page) None	21. No. Of Pages	22. Price N/A

This page intentionally left blank.

This page intentionally left blank.

Table of Contents

List of Tables	3
List of Figures	4
Executive Summary	6
1. Introduction.....	10
1.1. Background.....	10
1.2. Research Goals.....	11
1.3. Statement of Hypotheses.....	12
2. Literature Review.....	13
2.1. Physical Fundamentals.....	13
2.2. Current Methods to Estimate Bridge Pier Scour.....	20
2.3. The EFA/SRICOS Method	21
2.4. Generation of Synthetic Streamflow Hydrographs for Ungaged Sites.....	22
3. Methods.....	23
3.1. Site Selection	23
3.2. Analysis of Soil Properties.....	26
3.3. EFA Tests of Soil Samples	26
3.4. Hydrograph Methodology.....	29
3.5. Converting Discharge to Velocity Hydrographs.....	34
3.6. Predicting Bridge Pier Scour at Maryland Sites with SRICOS	34
4. Findings.....	39
4.1. Soil Characteristics and EFA Data	39
4.2. Synthetic Streamflow for Study Sites	45
4.3. Hydraulic Models.....	50
4.4. Bridge Pier Scour Estimates	51
4.5. Critical Velocity Tests	54
4.6. Use of Instantaneous Peak Discharges in Daily-Average Discharge Hydrograph	57
4.7. Discharge Order	59

5. Discussion.....	60
5.1. EFA Erosion Modeling.....	60
5.2. SRICOS Modeling.....	63
5.3. SRICOS Estimates of Scour Compared to HEC-18	64
6. Conclusions.....	65
6.1. Characterizing Maryland Soils with EFA.....	65
6.2. Method to Create Synthetic Hydrographs for Ungaged Sites in Maryland	66
6.3. Reduction of Predicted Scour Depth with SRICOS	66
6.4. Limitations of Current Approaches to Bridge Pier Scour in Cohesive Soils.....	67
6.5. Limitations of the EFA	67
6.6. Limitations of SRICOS.....	68
6.7. Limitations of the New Synthetic Hydrograph Technique	69
7. Recommendations for Future Research.....	70
8. References.....	72
Appendix A: Theory of Synthetic Hydrograph Technique.....	75
Appendix B: Erosion Rate Curves for Soil Samples	79
Appendix C: HEC-RAS Analysis of Study Sites	82

List of Tables

	Page
Summary Table. Comparison of Scour Depths	7
Table 3.1. Bridge Sites Selected for EFA-SRICOS Analysis.....	25
Table 4.1. Comparison Table of Shelby-Tube Soil Samples.....	40
Table 4.2. Instantaneous 100-Year Peak Flow (Ultimate Development)	49
Table 4.3. Comparison of Scour Depths Predicted by SRICOS and HEC-18.....	54
Table 4.4. Hydrograph Assumptions Used in the 15-Minute Discharge Experiment	58

List of Figures

	Page
Figure 2.1. Shields Diagram for incipient motion shear stress (Source: FHWA 2001, after Gessler 1971).....	14
Figure 3.1. MD 28 over Seneca Creek (existing bridge).....	24
Figure 3.2. MD 355 over Great Seneca Creek (existing bridge).....	24
Figure 3.3. MD 26 over Monocacy River (existing bridge).....	24
Figure 3.4. MD 7 over White Marsh Run (existing bridge).....	25
Figure 3.5. I-95/I495 over Potomac River (Woodrow Wilson Bridge) (rendered drawing of proposed bridge).....	25
Figure 3.6. The Erosion Function Apparatus (EFA).....	27
Figure 3.7. Mathematically-transformed discharges for Whitemarsh Run at White Marsh, Md., 1957-2002: (a) Natural logarithm of discharge; (b) Data with the annual cycle (mean and standard deviation) removed. In both (a) and (b), 40 years of observed data are superimposed.....	30
Figure 3.8. Interannual statistics of the natural-log-transformed discharge (lnQ) for Whitemarsh Run, showing parameters of the synthetic streamflow model.....	31
Figure 3.9. Example application of the Simulated Hydrograph method: (a) Recorded streamflow for 1969-1972, (b) Simulated streamflow for a generic four-year period, Whitemarsh Run at White Marsh, Md.....	33
Figure 3.10. Selected 160-day sequences from (a) Observed and (b) Simulated streamflow for Whitemarsh Run at White Marsh.....	33
Figure 4.1. Erosion Rate Curve, MD 26 over Monocacy River, Tube 1.....	42
Figure 4.2. Erosion Rate Curve, MD 26 over Monocacy River, Tube 2.....	42
Figure 4.3. Erosion Rate Curve, MD 355 over Great Seneca Creek, Tube 1, 2'-4'.....	42
Figure 4.4. Erosion Rate Curve, MD 355 over Great Seneca Creek, Tube 2, 6'-8'.....	43
Figure 4.5. Erosion Rate Curve, MD 28 over Seneca Creek, Tube B-3A, 5'-7'.....	43
Figure 4.6. Erosion Rate Curve, MD 28 over Seneca Creek, Tube B-3, 5'-7'.....	43
Figure 4.7. Erosion Rate Curve, MD 28 over Seneca Creek, Tube B-3, 7'-8.5'.....	43
Figure 4.8. Erosion Rate Curve, MD 7 over White Marsh Run, Tube 1, 1'-3'.....	44
Figure 4.9. Erosion Rate Curve, MD 7 over White Marsh Run, Tube 2, 1'-3'.....	44

Figure 4.10. Erosion Rate Curve, MD 7 over White Marsh Run, Tube 3, 1'-3'	44
Figure 4.11. Erosion Rate Curve, MD 495 over Potomac River, Tube 58'-60'	44
Figure 4.12. Parameters of the synthetic streamflow model, showing study sites in the range of calibration	47
Figure 4.13. Synthetic hydrograph model: annual cycle of mean, standard deviation, and day-to-day persistence (correlation) of $\ln(Q)$ for four study sites.....	48
Figure 4.14. SRICOS predicted pier scour, MD 7 over Whitemarsh Run.....	51
Figure 4.15. SRICOS predicted pier scour, MD 26 over Monocacy River	52
Figure 4.16. SRICOS predicted pier scour, MD 355 over Great Seneca Creek	52
Figure 4.17. SRICOS predicted pier scour, MD 28 at Seneca Creek	53
Figure 4.18. SRICOS predicted pier scour, I-95/495 at Potomac River (Woodrow Wilson Bridge).....	53
Figure 4.19. Neill's curves ("Suggested competent mean velocities for significant bed movement of cohesionless materials, in terms of grain size and depth of flow," showing extrapolation for finer particles (hand-drawn lines) and experimental results (dots).....	56
Figure 5.1. Soil samples undergoing EFA testing, showing greater scour at the tube walls than at the center and undulations deeper than 2 mm due to the removal of soil in chunks rather than by particles. All the Shelby tubes shown have outside diameter 76.2 mm. (Photos by MSHA).....	62

Executive Summary

Erosion of riverbed soil, also known as scour, around bridge piers can lead to catastrophic failures, loss of life, and great expense to the public. Current design methods to estimate bridge pier scour assume that the soil is non-cohesive (sand, gravel, or cobbles), and thus may provide conservative estimates of scour for piers that are placed in cohesive soil (clay). The physical behavior of scour in cohesive soils remains poorly understood, whereas there is a substantial body of knowledge about the power of flowing water to remove and transport non-cohesive sediments. This knowledge base is the main reason that non-cohesive scour methods are used for bridge pier design in a variety of soils. However, estimates based on assuming non-cohesive soil may be overly conservative, possibly resulting in unrealistically high scour depths and unnecessary costs.

This report describes and evaluates a set of hardware and software tools that have been developed to estimate bridge pier scour in cohesive soils: the Erosion Function Apparatus (EFA) and the Scour Rate In Cohesive Soils (SRICOS) method. The EFA is an apparatus designed to measure the erosion rate of a soil sample. SRICOS is a mathematical model that takes the EFA measurements as input and combines them with hydraulic data to predict the progression of pier scour in time. These tools were developed by J.L. Briaud and colleagues at the University of Texas, in cooperation with the Texas Department of Transportation; they have been tested on a number of sites in Texas. The State of Maryland is participating in a large-scale evaluation of the methods for soils and bridge crossings in other regions of the U.S.

Five bridge crossing sites in Maryland were identified for analysis. Soil cores were collected at the sites and analyzed using the EFA. This machine was designed to allow the investigator to determine the rate of erosion of a specific soil as a function of the velocity of water flow over the soil. The Erosion Function (scour rate as a function of velocity) determined in this manner is an essential input to the bridge pier scour prediction software, SRICOS. The SRICOS program also requires a long-term time series of daily flow velocity in the stream channel at the location of the bridge pier. Time series of artificial stream discharge were synthesized using a new method developed in the course of this study, which aims to represent the statistical patterns of daily discharge. Discharge values (cubic feet per

second) were transformed to velocity (feet per second) using hydraulic modeling software to create the required input data for SRICOS.

It was expected that the EFA would allow characterization of soils at Maryland bridge sites; that a regionalized regression-based synthetic streamflow model would provide physically-realistic sequences of discharge for input to the SRICOS program; and, finally, that the EFA-SRICOS method would predict less scour than the HEC-18 method.

The EFA was successfully applied to soil core samples from four of the five selected Maryland sites to determine Erosion Functions for the soils at these locations. Due to technical difficulties, testing was only partially successful for the fifth site. Prediction equations were developed to determine the parameters required to generate long synthetic time series of discharge for ungaged basins in the Maryland Piedmont and Coastal Plain; the equations are based on watershed properties that can be directly determined from GISHydro2000, a customized ArcView-based hydrologic analysis software tool developed by Dr. Glenn Moglen of the University of Maryland for the MSHA.

For three study sites, SRICOS scour predictions were approximately 60% of the depth predicted by the current state-of-the-art method (HEC-18, FHWA 2001), which assumes non-cohesive soil and is based on a measured particle size distribution (Summary Table). In one case, the SRICOS method predicted only about 2% of the non-cohesive method's predicted depth. In examining these results, three important notes must be made. First, the SRICOS results reflect physical tests of erosion of real soil, and not assumptions based on scour of cohesionless soil. Second, the two methods are based on different hydraulic inputs: the HEC-18 calculations are based on a single value of discharge, the 100-

Summary Table. Comparison of Scour Depths

Site	SRICOS Scour (ft)	HEC-18 Scour (ft)	SRICOS Scour as a % of HEC-18 Scour
MD 7 over White Marsh Run	3.2	5.4	59%
MD 28 over Seneca Creek	0.2	8.4	2
MD 355 over Great Seneca Creek	2.3	4	58
MD 26 over Monocacy River	7.7	12.4	62
Woodrow Wilson Br. (Potomac River)	26.5 (incomplete)	30-46	72 (incomplete)

year instantaneous peak flow under conditions of ultimate development in the watershed, whereas the SRICOS calculations use observed or synthetic time series of daily discharge based on past and present conditions, with the 100-year peak flow arbitrarily inserted into the time series in several cases. These differences are discussed in the report. Finally, the comparisons in this study were made between two prediction methods, and neither has been compared to field data of scour.

In the context of evaluating the tools and methodology for use in the state of Maryland, it is important to note that the EFA-SRICOS method is an emerging technology that shows promise for application to some Maryland bridge sites. The current study included only five sites, limiting the amount of data collected and the conclusions to be drawn from the data. The method is currently being tested by several state Departments of Transportation; the results of these studies, and issues identified, will help to refine, improve, and validate the method.

Several issues and possible limitations of the EFA/SRICOS method were identified in the course of this study. These issues include the fact that very few bridge crossing sites in Maryland possess the combination of spatially continuous cohesive soil and in-channel (rather than floodplain or overbank) location of the piers for which the method seems best suited. Maryland soils are highly variable, even within the spatial scale of a single bridge span, and it may be unwise to apply the erosion rate determined from one or several cores over an entire site. In addition, a number of theoretical questions were raised about the method's assumptions concerning initiation of motion in cohesive sediments and the appropriateness of extrapolating results from a small core of material in a flume to the scale of a bridge pier. These issues and limitations are discussed in more depth in the report. Nonetheless, the EFA represents a novel approach to quantifying the erodibility of cohesive soils.

More study is required to determine what is the most appropriate streamflow time series with which to drive the SRICOS scour-prediction model. The objective is to design a bridge to be stable under conditions of "worst-case" scour. When evaluating a new method for estimating scour, MSHA's design philosophy is to err on the side of safety, or to over-predict rather than under-predict scour depths. In that spirit, a "worst-case" design

hydrograph may be more appropriate than a “realistic” hydrograph in developing the hydrologic input for the SRICOS method.

The MSHA develops the hydrology and flood estimates for a bridge based on the ultimate development in the watershed. Neither the recorded, historic streamflow hydrographs recommended by the EFA/SRICOS authors nor the method of synthetic streamflow time series developed in this study reflect changes in the statistics of the discharge at the bridge crossing as the watershed undergoes future land-use change during the lifetime of the structure. The relevance of this issue to pier scour prediction underscores MSHA’s commitment to ongoing hydrologic research.

One recommendation of this study is that the MSHA should establish a long-term monitoring program for the bridge piers analyzed, using photographs and measurements of any scour holes that develop, in order to test the predictive value of the EFA-SRICOS method, and other bridge pier scour prediction methods, in this region.

1. Introduction

1.1. Background

Scour is the removal of soil due to the forces created by flowing fluid. When scour occurs at a structure such as a bridge, the scour may undermine the foundations, resulting in structural failure. This was the cause of the bridge failure over Schoharie Creek in 1987, which resulted in the loss of 10 lives, and the 1989 Tennessee Hatchie River bridge failure in 1989, which resulted in eight lives lost. Although these are extreme cases, these failures help to illustrate scour's potentially devastating effects.

Since the failure of these two bridges in 1987 and 1989, the Federal Highway Administration has mandated scour prevention on all federally-funded road projects. Typically, in order to prevent undermining of foundations, most bridge foundations are designed to extend well below the estimated scour depth.

There has been much research done in the field of scour in coarse or sandy soils, but relatively little comparable research of scour in cohesive soils such as silts and clays. Sandy soils are known to erode particle by particle while cohesive soils usually erode in clumps rather than individual particles. However, the bonding mechanism of cohesive soils is little understood from one cohesive soil to another. Studies reveal that soil type, water temperature, salinity, plasticity index, liquid limit, and molecular bonding are among some of the parameters that may have some effect on the bonding of cohesive soils. Other studies report results that appear to contradict some of these findings. Because this bonding is so complex, no set of equations to predict scour depths in cohesive soils has been widely accepted.

The Federal Highway Administration has recommended use of the HEC-18 pier scour equations (FHWA 2001) to estimate maximum scour depths at structures. However, these equations were developed to estimate scour in non-cohesive soils. The prevailing assumption is that cohesive soils will scour to the same depth as non-cohesive soils, although it will take longer to reach the same scour depths. Using non-cohesive equations to provide a conservative (but unquantified) margin of safety for foundation depths in cohesive soils may

result in unnecessary expense if scour depths in cohesive soils do not reach the maximum scour depths predicted by the non-cohesive equations.

A new method called Scour Rate in Cohesive Soils (SRICOS, Briaud et al. 1999, 2001a,b) attempts to empirically estimate maximum cohesive soil scour at bridge piers. The SRICOS method relies on measuring the rate of scour for site specific soils in the laboratory using a modified flume called an Erosion Function Apparatus (EFA). The EFA determines the amount of erosion for a given velocity. In concept, the EFA allows the user to determine directly the critical shear stress of the in situ soil. This information is combined with both the calculated velocities found at the bridge pier site and a stream velocity hydrograph of predetermined time length to predict the scour depth over a desired time period. Since this method does not rely on soil composition or other indirect soil properties, it does not delve into the reasons for the soil cohesiveness or the conditions that will produce scour in the soil other than the critical shear stress required for particle movement. Water temperature and salinity and soil properties such as the clay-silt ratio are not included as input parameters.

SRICOS is the only known method currently available that estimates scour depth as a function of time. Under the prevailing assumption that cohesive soils require more time to reach their maximum scour depths than non-cohesive soils, if a time factor could be incorporated into the scour equations then it might be possible to design foundations that need only be as deep as the scour depth that can be expected over the life of the structure. A driving force for bridge owners to adopt more accurate methods for estimating scour would be the potential financial savings due to reduced foundation depths when building new structures.

1.2. Research Goals

The goal of this study is to evaluate Briaud et al.'s (1999, 2001a,b) method to predict bridge pier scour in cohesive soils in terms of its applicability to bridge crossing sites in Maryland. The method, known as EFA-SRICOS, was developed at the University of Texas, using soils and streams in Texas. The current study is part of a larger project to evaluate the method in different regions of the country. The study consisted of three stages: (1) using the Erosion Function apparatus (EFA) to characterize cohesive soils at selected bridge crossing sites in

Maryland; (2) developing a method to generate synthetic discharge hydrographs for ungaged sites in Maryland to provide the required inputs to SRICOS; and (3) based on inputs from the first two stages, using the SRICOS method to predict bridge pier scour at the selected sites.

This study applies and evaluates the EFA-SRICOS method for conditions at bridge piers in the state of Maryland. It follows the procedures outlined in reports by Briaud, et al. (1999; 2001,a,b; 2003) for the Texas Department of Transportation Construction Division. The EFA-SRICOS results are compared to current methods, which are based on non-cohesive soils and instantaneous peak flow under conditions of ultimate development in the watershed, and which do not calculate the time frame for the occurrence of the ultimate scour depth.

1.2. Statement of Hypotheses

Expected outcomes of this research were as follows:

- (a) The use of the Erosion Function Apparatus would allow characterization of the erodibility of cohesive soils at bridge crossing sites in Maryland.
- (b) The statistical analysis of gaged streamflow would reflect the effects of measurable watershed characteristics on magnitude, timing, and persistence of high flow events (scour-causing events) and allow the synthesis of realistic long time series of discharge for ungaged watersheds.
- (c) Using the same hydrologic/hydraulic inputs, the EFA/SRICOS method would predict less scour than current methods that are based on non-cohesive soils.

2. Literature Review

2.1. Physical Fundamentals

Flowing water over sediment exerts forces on streambed sediments that tend to move or entrain the sediments. The entraining forces have two components: the tangential force, drag, and the normal force, lift. Drag results from viscous stresses at low velocities but at high velocities the pressure differential between the upstream and downstream face of the particle is the principle force moving the particles (Leopold, 1994). Finer sediments composed of cohesive soils, such as silt and clay, resist entrainment mainly by cohesion.

Critical condition is defined as the point when the fluid force acting on a grain of sediment or on particles of cohesive sediment reaches a value that puts the particle into motion. Particle movement first appears erratic and is the result of the unstable grain position relevant to other particles. At some point movement becomes more general, determining the point at which the critical condition is reached. Data available on critical shear stress are based on what seem to be subjective definitions of critical conditions. However, observers asked to decide when general movement has occurred, will pick a point that is within a few percent of the same velocity, (Henderson 1966).

Early Shear Stress Studies. Flume experiments on critical shear stress for non-cohesive sediments show that the motion of sediment grains at the bed is highly unsteady and non-uniformly distributed over the bed area.

The drag force is predominant in turbulent flows when the Reynolds number ($D_s V/\nu$) is high (where D_s is the particle diameter, V is velocity, and ν is kinematic viscosity). In laminar flow the shear force is predominant and the Reynolds number is small. The ratio of the forces that move a particle to that of the forces that resist movement is:

$$\frac{\tau_0}{(\gamma_s - \gamma)D_s} \tag{2.1}$$

where: τ_0 = average shear stress

γ = specific weight of water

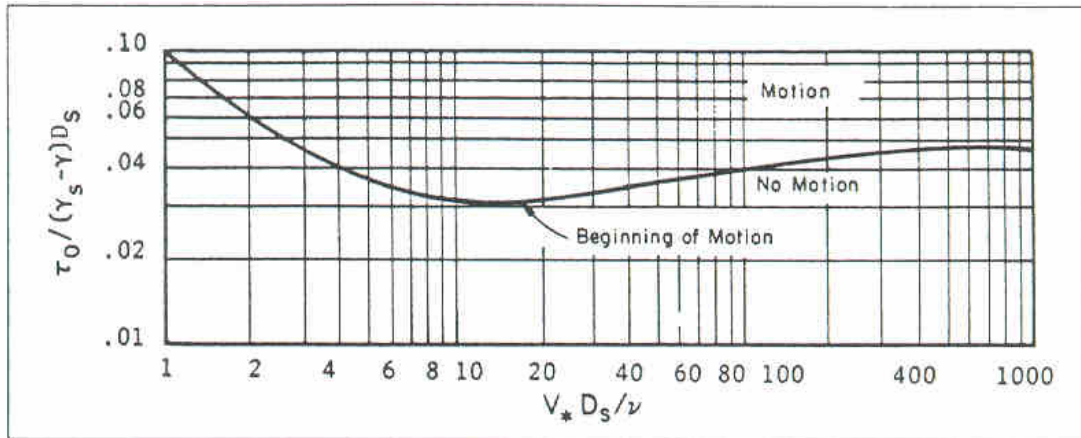


Figure 2.1. Shields Diagram for incipient motion shear stress (Source: FHWA 2001, after Gessler 1971).

γ_s = specific weight of the sediment

D_s = diameter of sediment particle

Shields' experiments on incipient motion in the 1930's determined the relationship between the Reynolds number, VD_s/ν , and $\tau_0/(\gamma_s - \gamma)D_s$, known as the Shields relation. His experiments led to the development of the widely-accepted Shields diagram to determine the incipient motion shear stress (Fig. 2.1) (FHWA 2001).

Critical Velocity. Particle movement in steady, uniform flow begins when the shear stress equals the resistance forces on the particle. The velocity profile for a two-dimensional free-surface flow over a flat sediment bed is given by

$$U/U^* = a_r + 5.75 \log y/k_s \quad (2-2)$$

where

U = the velocity at distance y above the bed

U^* = friction velocity

k_s = the characteristic roughness of the sediment size

a_r = a function of the boundary Reynolds number

Equation (2-2) shows that if two flows of different depth have flat beds of identical sediment and the same bed shear stress, the velocities at any distance y above the bed will also be the same in the two flows. However, because the mean velocity occurs at y equal to a constant fraction of the depth, the deeper flow will have the larger mean velocity. To determine the scouring action of the water at the bed, the mean velocity and depth of the bed must also be given. The bed condition can also be specified by a velocity at a given value of y . The advantage of using shear stress to identify critical conditions is that only one variable is necessary.

Relations between velocity, depth, and particle resistance have been developed from equating shear stress to resistance. The development summarized below follows FHWA (2001) Appendix C, and is presented in metric (SI) units. The average bed shear stress can be found by the equation:

$$\tau_0 = \gamma RS \quad (2.3)$$

where

γ = unit weight of water

R = hydraulic radius

S = slope

For wide channels, y may be substituted for R . If the Mannings equation,

$$V = \frac{R^{2/3} S^{1/2}}{n} \quad (2.4)$$

(where n is Manning's roughness coefficient) is used to find the slope, then Eq. (2.3) becomes :

$$\tau_0 = \rho g y S_f = \frac{\rho g n^2 V^2}{y^{1/3}} \quad (2.5)$$

The Shields relation can be used to determine the relation between the critical shear stress

and the bed material size for incipient motion. That relation is:

$$\tau_c = K_s(\rho_s - \rho)gD_s \quad (2.6)$$

where

D_s = diameter of particle

K_s = Shield's coefficient

If the applied shear stress equals the critical shear stress,

$$\tau_0 = \tau_c \quad (2.7)$$

then

$$\frac{\rho g n^2 V^2}{y^{1/3}} = K_s(\rho_s - \rho)gD_s \quad (2.8)$$

Equation (2.8) can be rearranged to find the velocity associated with initiation of motion of particle size D :

$$V_c = \frac{K_s^{1/2}(S_s - 1)^{1/2} D_s^{1/2} y^{1/6}}{n} \quad (2.9)$$

where

S_s = specific gravity of the sediment.

Using $K_s = 0.039$, $S_s = 2.65$ (specific gravity for quartz), and $n = 0.041 D^{1/6}$ (for D in m),

$$V_c = 6.19 D_s^{1/3} y^{1/6} \quad (2.10)$$

where D_s and y are given in m, and V_c in m/s.

Equation (2.10) gives the critical velocity, above which bed material of size D and smaller will be transported; this equation assumes steady, uniform flow. FHWA (2001) recommends its use to find the critical depth and size for incipient motion based on the Mannings equation, specific gravity of the particles and the Shields parameters.

Lift on Particles. As reported by ASCE (1977), Einstein and El-Samni (1949) measured the difference in mean static pressure in sediment beds at the level of the bottom of the top layer of sediment and at the wall of the channel at the top of the top layer of sediment. In these experiments, the velocity was less than the critical velocity and no sediment moved. Their measurements yielded a pressure difference or lift pressure, Δp , on the grains given by

$$\Delta p = 0.178(0.5\rho u_o^2) \quad (2-11)$$

where

u_o = the velocity at the height of the d_{35} particle above the bed

d_{35} = size of grains for which 35% by weight of the bed material is finer

The Reynolds values in the experiments used to obtain Eq. (2-11) were approximately 50,000. Therefore, the lift pressure given by Eq. (2-11) should be valid only for rough boundaries.

Scour in Cohesive Soils. A literature search reveals that there is relatively little research of scour in cohesive soils. The factors that result in cohesive soils seem to be many and varied as reported by a number of researchers over the years. It is clear from the research that sediment properties that determine its resistance to erosion are not completely defined.

According to ASCE (1968), Dunn (1959) determined the critical shear stress for sediments ranging from sand to silty clay taken from several channels in the Western U.S. He applied a submerged jet of water directed vertically downward onto sample sediments. He concluded that increasing clay content increases the critical shear stress. Further, ASCE reports that Smeardon and Beasley (1961) determined the critical shear stress for 11 cohesive soils. They concluded that the plasticity index and the percentage of clay in the soils had an effect on the shear stress. However, these conclusions were disputed by Flaxman (1963),

who reported that, although some researchers had found a relation between high plasticity index and high resistance to erosion, he examined several natural channels and found that low- or no-plasticity soils exhibited high resistance to erosion. Flaxman examined soil permeability and unconfined compression tests as indicators of erodibility of clay; however, it is difficult to make an argument supporting why these would be reliable indicators.

Grissinger and Asmussen (1963) found that the erosion resistance of clay soils varied with the type and amount of clay minerals, orientation, bulk density and antecedent water content and the water temperature.

The ASCE (1977) report described research by Abdel-Rahmann (1964) who studied the erosion resistance of clayey sediments. The clay used in these experiments was high in silicate content (more than 90%) and of a type that swells when it absorbs water. The conclusion was that the erosion process was independent of shear stress and was related to the swelling of the clay.

Grissinger (1966) studied the properties of certain clays that are resistant to erosion. He concluded that the type and amount of clay present in the soil, as well as the orientation of the clay particles and the temperature of the eroding water, all vary the ability of the cohesive soil to resist erosion.

Kuti (1976) found that the ultimate volume of soil scoured, regardless of the percentage of clay mineral present, was the same. However, the in-situ void ratio determined the length of time it took to reach the equilibrium scour depth. He also found that the percent clay in a soil and its plasticity index can be used as indicators of soil resistance to erosion.

Kamphuis (1989) studied the influence on erosion in a cohesive bed of the non-cohesive material carried by the streamflow. The sediment transport characteristics of an eroding fluid containing a granular material greatly influences the erosion of the cohesive material. He found this to be true in all cases except in absolutely clear water. Kamphuis further states that if granular materials are present in the stream or a granular material overlays a cohesive soil in a discontinuous layer, the design should be based on the sediment transport characteristics of the granular material.

Briaud et al (1999) discussed a study of cylindrical pier scour in cohesive soils that predicted scour depth versus time for a constant velocity flow. Shelby tube soil samples are tested in an Erosion Function Apparatus, EFA, to obtain an erosion rate versus shear stress

curve. This method of scour prediction in cohesive soils is discussed in depth later in this chapter.

Guyen et al. (2003) discussed a simplified theory of bridge scour in cohesive soils over time in clear water based on Briaud's (1999) "scour rate in cohesive soils" concepts. Guyen et al. developed a differential equation based on Briaud's empirical rate of erosion for the dependence of the flow depth at time t .

Molinas et al. (1996) studied the magnitude and geometry of the equilibrium local scour at a bridge pier in cohesive soil. Their results showed in part that the scour depth decreased as the clay/sand ratio increased up to 40%. Beyond this clay content, other factors such as compaction, water content, etc. become more critical to the ability of the soil to resist erosion. They also found that the higher the clay content, the longer it takes to reach the equilibrium scour depth and the steeper the slope of the scour hole. They also argued that as the initial soil water content decreases the scour depth decreases. (This study is not directly applicable to in situ clays because Molinas made his own clay and let it set up for only a few days as opposed to in situ clays that have been compressed by natural forces.)

Annandale's (1999) Erodibility Index Method estimates pier scour in rock and other scour-resistant soils. The method is based on stream power (average velocity times bed shear stress) and soil resistance to erosion. The erosion resistance is defined by the Erodibility Index, a geo-mechanical quantifier. Scour stops when the erosive power required to scour exceeds the available erosive power.

Ansari et al. (2002) state that there is little known about the effect of cohesive material on pier scour. As other researchers have found, the point at which a cohesive material is eroded is difficult to predict because it varies with the type and percentage of the clay content, compaction and/or consolidation. Their monitoring of scour holes revealed that sediments with clay content between 5% and 10% scoured first from the sides of the pier, then the scour holes propagated upstream along the sides of the pier and met at the nose of the pier. The scour depth increased rapidly and created the deepest scour hole at the pier nose.

In their studies of erodibility of cohesive streambeds in the Midwestern U.S., Hanson and Simon (2002) found that correlations to individual soil characteristics such as plasticity index, undrained shear strength and gradation were poor and can only be rough indicators of

erodibility. They agreed with the Briaud (2001a) conclusions that there is no generally accepted correlation between measured soil parameters and erodibility and thus a direct measurement method is better.

2.2. Current methods to estimate bridge pier scour

Current methods for determining scour at bridge piers in cohesive soils rely on equations for scour in sandy soils, based on the assumption that cohesive soils will scour to the same depth as non-cohesive soils but will take much longer to reach the maximum scour depth. This section summarizes these methods.

Melville and Chiew (1999) conducted experiments on uniform sands to develop an equation for equilibrium scour depth at a bridge pier as a function of time in clear water scour. They concluded that equilibrium scour depth is approached asymptotically, that scour depths after 10% of the time to equilibrium has passed achieved 50% to 80% of the equilibrium scour depth, and that time to equilibrium is a function of flow intensity, flow shallowness and sediment size. Their equations can be used to estimate the scour depth at any stage of the scour hole development.

HEC-18 (FHWA 2001) is a method of calculating scour in non-cohesive soil (sand, gravel, cobbles). According to the HEC-18 manual, the foundation of scour equations is conservation of mass in sediment transport: there must be an equilibrium of sediment and water flow into and out of a cross section. As the scour hole enlarges and increases the flow area, the shear stress and average flow velocity decrease. This describes the point of maximum scour depth in the case of live bed scour. In the case of clear water scour no sediment is transported into the cross section and the maximum scour depth is reached when the critical shear stress of the bed material is reached.

HEC-18 uses a modified Colorado State University (CSU) equation recommended by FHWA Technical Advisory T5140.23 dated October 28, 1991. The modification includes coefficients for the effect of bed form and bed size material. When the equation was compared to USGS field data, it was found to produce conservative scour depths that provided a built-in margin of safety. The resulting HEC-18 equation is used for both clear water and live-bed pier scour and predicts the maximum pier scour depths. The equation is:

$$\frac{y_s}{y_1} = 2.0K_1K_2K_3K_4\left(\frac{a}{y_1}\right)^{0.65} Fr_1^{0.43} \quad (2-12)$$

where:

- y_s = scour depth
- y_1 = flow depth directly upstream of the pier
- K_1 = correction factor for pier nose shape
- K_2 = correction factor for angle of attack of flow
- K_3 = correction factor for bed condition
- K_4 = correction factor for armoring by bed material size
- a = pier width
- Fr_1 = Froude Number directly upstream of the pier = $V_1/(gy_1)^{0.5}$
- V_1 = mean velocity of flow directly upstream of the pier
- g = acceleration of gravity (9.81 m/s²) (32.2 ft/s²)

Equation (2-12) applies to scour in non-cohesive soil (sand, etc.). The correction factors (K_1 through K_4) are based on bridge geometry and stream bed characteristics and can be determined from look-up tables in the HEC-18 manual.

2.3. The EFA/SRICOS method

A study of pier scour in cohesive soils sponsored by the Texas Department of Transportation (Briaud et al. 2001b) proposed a method to predict scour as a function of time. The method combines information on soil properties obtained from a modified flume called the Erosion Function Apparatus, EFA (Briaud et al. 2001a), the flow velocity in front of the pier obtained from a hydraulics software program such as HEC-RAS, a discharge hydrograph obtained from USGS gage sites, and their SRICOS software (Briaud et al. 1999). The underlying concept of this study is that, since cohesive soil bonding is so complex and not easily understood, a better approach is to remove site-specific soils in as undisturbed condition as possible and through direct erosion tests determine the critical shear stress of the soil. This information, combined with a velocity hydrograph of the site, should give a more

realistic estimate of the maximum scour depth. The EFA-SRICOS methods are the focus of this study and are discussed in detail in Chapter 3.

2.4. Generation of Synthetic Streamflow Hydrographs for Ungaged Sites

The SRICOS method requires as input a series of daily average velocities at the pier location. The velocities can be computed from records or estimates of stream discharge, using hydraulic methods. If long-term discharge measurements are available at a bridge site, these measured discharges can be used as input to SRICOS. The SRICOS manual recommends the use of USGS streamflow records, if they are available.

In order to apply SRICOS to any bridge crossing site, methods must be developed to extend measured streamflow records that are too short to predict ultimate scour, and to create synthetic discharge hydrographs for locations that do not have gage records. Salas (1993) describes a method to produce realistic synthetic discharge hydrographs by taking into account the seasonally varying interannual mean and standard deviation of streamflow, as well as the tendency of the streamflow to persist at a given level from one day to the next.

Briaud et al. (2002) propose a probabilistic (or risk analysis) method to estimate design-life scour depth using synthetic future streamflow hydrographs as input to the SRICOS method. Their streamflow generation technique consists of characterizing the daily discharge by a lognormal distribution. Their method assumes that the mean and standard deviation of daily discharge are constant throughout the year and further, that each day's flow is independent of the previous day's value.

3. Methods

Five test sites with cohesive soils at the bridge piers were selected to test the SRICOS method for pier scour under Maryland conditions. Samples from the sites were analyzed using the Erosion Function Apparatus (EFA) to obtain the required entry data for the SRICOS program. Four of the five sites are ungaged; therefore, a synthetic hydrograph procedure was developed to produce the required time series of discharge for input to the SRICOS program. The scour depths predicted by SRICOS were compared to scour depths obtained from the commonly used Federal Highway Administration HEC-18 method (FHWA 2001). This chapter describes the procedures used for each of these steps.

3.1. Site selection

Appropriate sites for this study need to have cohesive soils and a bridge crossing with piers in the channel. Identifying sites turned out to be a greater challenge than expected. Maryland State Highway Administration (MSHA) geotechnical engineers identified areas in Maryland most likely to have cohesive soils. According to these sources, these soils are primarily in the Piedmont and Coastal Plain Regions of Maryland extending through Montgomery, Frederick, Howard, Anne Arundel, and Carroll counties.

All MSHA-owned bridges in the selected region were identified and the soil boring logs scrutinized for clay material at the piers. The selected study sites were MD 28 over Seneca Creek (Fig. 3.1), MD 355 over Great Seneca Creek (Fig. 3.2.), MD 26 over Monocacy River (Fig. 3.3), MD 7 over White Marsh Run (Fig. 3.4), and I-95/I-495 over the Potomac River a.k.a. Woodrow Wilson Bridge (Fig. 3.5). The study sites are summarized in Table 3.1.

In addition, the ideal study site would be characterized by observed, quantified bridge pier scour, which would allow assessment of prediction accuracy. For the four existing bridges, however, MSHA inspection records did not indicate any pier scour to date.



Figure 3.1. MD 28 over Seneca Creek (existing bridge).



Figure 3.2. MD 355 over Great Seneca Creek (existing bridge).



Figure 3.3. MD 26 over Monocacy River (existing bridge).



Figure 3.4. MD 7 over White Marsh Run (existing bridge).



Figure 3.5. I-95/I495 over Potomac River (Woodrow Wilson Bridge) (rendered drawing of proposed bridge).

Table 3.1 Bridge Sites Selected for EFA-SRICOS Analysis

Site	Water Crossing	County	Number of Samples
MD 28	Seneca Creek	Montgomery	4
MD 355	Great Seneca Creek	Montgomery	2
MD 26	Monocacy River	Frederick	2
MD 7	Whitemarsh Run	Baltimore	4
I-95/495	Potomac River (Woodrow Wilson Bridge)	Border of Prince George's County and Virginia.	2

It is MSHA policy to minimize channel scour at bridge crossings by placing bridge piers in the overbanks where possible. Consequently, three of the bridge sites selected (MD 28 over Seneca Creek, MD 355 over Great Seneca Creek and MD 7 over White Marsh Run) have piers in the overbanks. This policy required modifications to be made in the SRICOS method that are detailed later in this chapter.

3.2. Analysis of Soil Properties

Samples were obtained using an ASTM 1587 AASHTO 207 standard Shelby tube with a 76.2 mm outside diameter. If a sample could not be taken near the pier, then the sample was taken from the overbank in the same soil layer as the pier. MSHA personnel collected Shelby tube samples from each site and the sample soil trimmings were tested by the MSHA soils lab for identification of soil type, D_{85} , D_{50} , D_{35} , Atterberg Limits (Plasticity Index, Plastic Limit, Liquid Limit), and the content of gravel, sand, silt and clay. The Atterberg Limits are used to describe the ability of a fine-grained soil to absorb water. The plastic limit defines the water content at point of transition of the soil from semisolid to plastic state. The liquid limit defines the water content at the point of transition of the soil from plastic to liquid state.

3.3. EFA Tests of Soil Samples

As described in the SRICOS Research Report 2937-1 (Briaud, 1999) the sample tube was placed on the EFA piston, the soil sample trimmed flush to the top of the tube, and then fed through a circular hole in the flume, that is sealed with an O-ring, until the tube was flush with the bottom of the flume. The flume is a 4" x 2" rectangular pipe with flow straighteners at the upstream end to reduce turbulence. A photograph of the EFA is shown in Fig. 3.6.

Once the tube was securely set in place and the water pump was turned on, the velocity was set to the desired speed and the sample was pushed into the flow 1 mm. As the sample eroded, the 1-mm protrusion of the soil sample in the flow was maintained by manually advancing the piston. The sample was tested for 1 hour or 50mm of erosion,

whichever came first. At the end of the test, the sample was removed from the flume, re-trimmed flush to the tube and the procedure was repeated for up to 8 tests at velocities of 0.3m/s, 0.6m/s, 1m/s, 1.5m/s, 2m/s, 3m/s, 4.5m/s, and 6m/s. Erosion results from the 6m/s velocity were regarded as unreliable due to the opaqueness of the water and the inability to see the sample and push it in a timely manner. The erosion and calculated shear stress were recorded for each velocity. The data obtained was used to plot the erosion rate vs. velocity curve and the shear stress vs. velocity curve for each soil sample; this information is required for the SRICOS program. The erosion recorded for each test was used to calculate the erosion rate in mm/hr. The shear stress at the selected critical

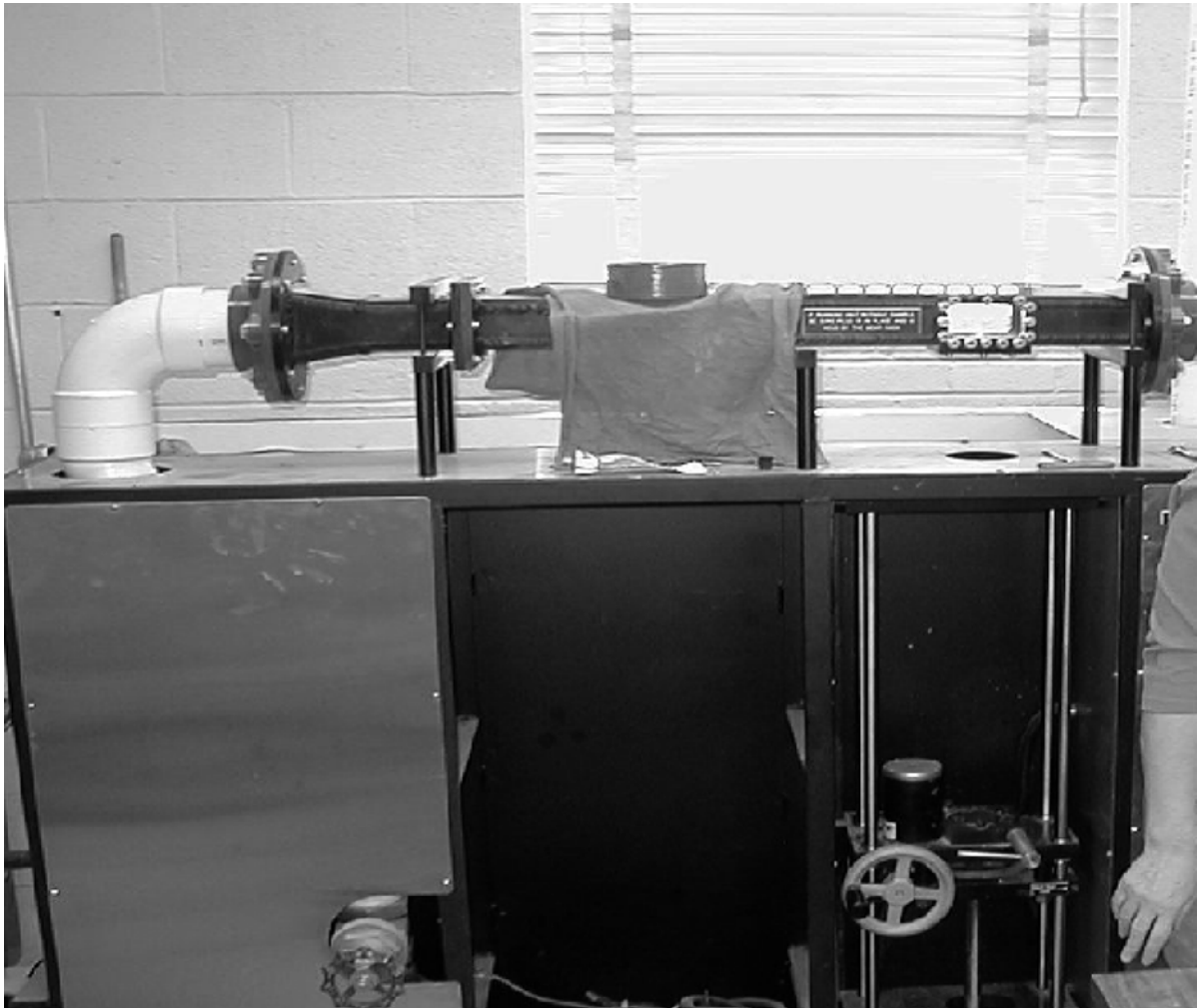


Figure 3.6. The Erosion Function Apparatus (EFA).

shear stress was determined according to the SRICOS method by calculating the shear stress from the Moody Chart for pipe flows,

$$\tau = \frac{1}{8} f \rho V^2 \quad (3-1)$$

where: V = mean flow velocity

ρ = mass density of water

f = friction coefficient whose value corresponds to the Reynolds number, Re , and the soil surface roughness ε/D on the Moody Chart.

The Moody Chart was used to obtain f from the calculated Reynolds number and ε/D . The Reynolds number was computed as VD/ν , where D was the pipe diameter, V was the mean water velocity in the pipe, and ν was the kinematic viscosity of water (10^{-6} m²/s at 20° C). The ratio ε/D represents the pipe roughness where ε was the average height of the roughness elements on the pipe surface. The EFA pipe is rectangular in cross section; the diameter D was calculated as $4 \cdot \text{Area} / (\text{Wetted Perimeter})$ which equals $2ab/(a+b)$, where a and b are the dimensions of the pipe. After the shear stress was calculated, the erosion vs. shear stress curve was obtained for each test sample.

It should be noted that the SRICOS method for determining ε/D uses the roughness element, ε , equal to 1/2 of the D_{50} based on the assumption that only half the particle protrudes into the flow. However, it was decided that a more relevant roughness would be that of the pipe surface roughness, since the pipe walls constitute approximately 65% of the perimeter of the cross section compared to the soil sample that comprises approximately 35% of the perimeter of the same cross section. While this is a minor change causing no more than a 10% difference in f , it was judged to be more indicative of the roughness factors controlling turbulence in the pipe.

The critical shear stress for each layer of soil found at the site was determined and this shear stress as well as the depth of the soil layer it came from, were entered into the soil data window of the SRICOS program.

3.4. Hydrograph Methodology

Generating Synthetic Hydrographs for Ungaged Sites in Maryland

The SRICOS method requires a time series of flow velocity, which is generally obtained from the time series of discharge using hydraulic models. Briaud et al. (1999) suggest using average daily discharge data downloaded from the USGS stream gage website. Most Maryland streams do not have gages at bridge sites. A search of USGS gages found that there were gages on four of the streams or rivers crossed by the five bridges selected, but that three of these gages were too far away from the sites to be of meaningful use. Only one of the study locations had a stream gage at the site (MD 7 at White Marsh), and the 40-year flow record at that site was not long enough to include the extreme-value flows that would result in an ultimate scour depth. Thus, it was necessary to develop a procedure to generate long, realistic sequences of daily average flow, both for the gaged site and the ungaged sites, as input to the SRICOS program.

The procedure developed to generate time series of synthetic streamflow is summarized here, using Whitemarsh Run at White Marsh, Md., as an example. Theoretical details are provided in an Appendix to this report.

USGS streamflow data were obtained for a number of gaging stations throughout the different geological provinces of Maryland. Only stations with a record of at least 30 years were selected. The discharge (Q) data were first converted to the natural logarithm ($\ln Q$) of daily flow.

When considered across years, daily discharge records in Maryland show strong seasonality in their average value and their variability around the average. In Figure 3.7(a), forty years of natural-log-transformed streamflow are superimposed; a sine-wave pattern is apparent, with a maximum at about Day 80 (mid-March) and a minimum at about Day 230 (mid-July). Additionally, the flows exhibit a greater range of values in the summer than in the winter. These interannual patterns are captured by computing, for each day of the year, an average value and a standard deviation across all the years of record. For example, 40 years' values of flow on April 1 are analyzed for their average and standard deviation.

Each daily natural log discharge is standardized by subtracting out the interannual average, then dividing by the interannual standard deviation for that day. The result is a time series of data with a mean of zero and standard deviation of one. The results of this standardization for Whitemarsh Run are shown in Figure 3.7(b); in the standardized data, the seasonal sine wave and differences in range are no longer evident.

In addition to average and standard deviation that vary throughout the year, the daily discharge is characterized by a degree of persistence, that is, the tendency for high discharge to be followed by high discharge, and likewise for low values. This tendency for today's flow to be similar to yesterday's flow is quantified by a one-day correlation term. The correlation was computed from the time series of standardized data for all years; for example, the statistical correlation between flow on March 31 and April 1 is computed across 40 years to give the one-day correlation for April 1.

The computed year-long series of interannual averages, standard deviations, and one-day correlation were curve fit using a cosine-wave model. Any cosine wave is described by three parameters: its central value, its amplitude, and its time of maximum.

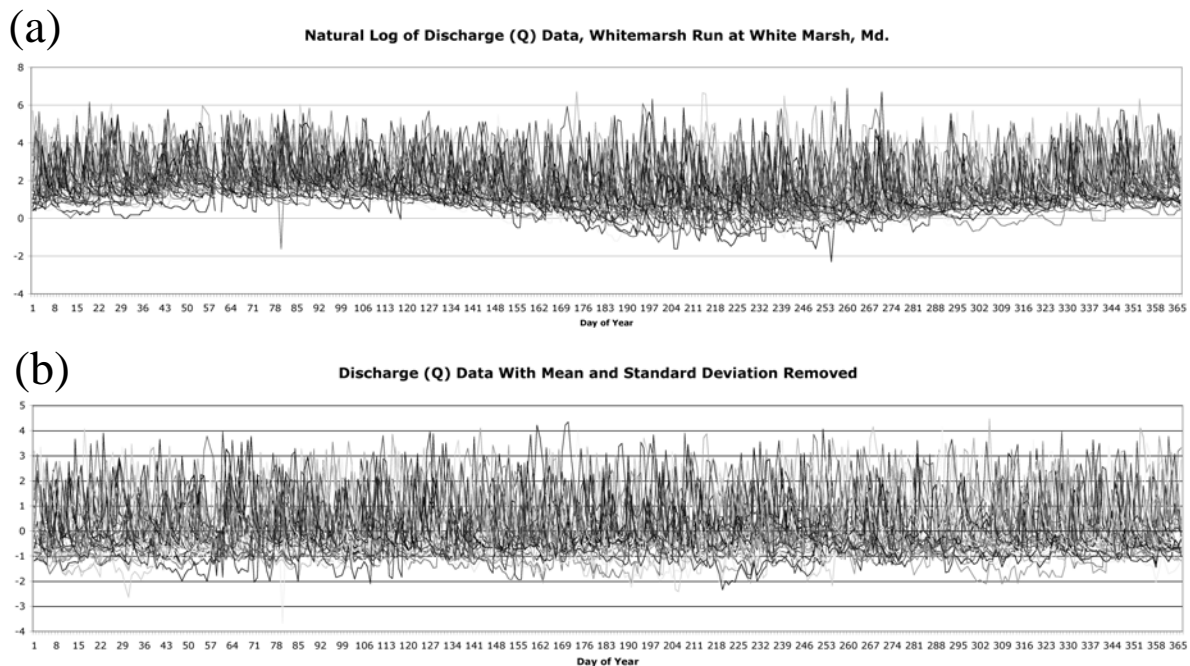


Figure 3.7. Mathematically-transformed discharges for Whitemarsh Run at White Marsh, Md., 1957-2002: (a) Natural logarithm of discharge; (b) Data with the annual cycle (mean and standard deviation) removed. In both (a) and (b), 40 years of measured data are superimposed.

The computed interannual statistics, their cosine-wave curve fits, and the parameters for Whitemarsh Run are shown in Figure 3.8; the “A” terms describe the central values of the cosine waves, the “B” terms their amplitudes, and the “ τ ” terms their time of maximum, measured from day 0. In general, the one-day correlation did not exhibit noticeable seasonal variation; therefore, it was modeled as a constant, A_3 .

The time series of discharge for each gage was analyzed as described above. The parameters ($A_1, B_1, t_1, A_2, B_2, t_2, A_3$) were estimated for 27 gaged sites in the Maryland Piedmont and 27 in the Coastal Plain. Using multiple linear regression, each parameter was expressed in terms of predictors that can be estimated for any watershed, whether gaged or not, using GISHydro2000. The predictors that were found to be useful included, for example: the natural log of drainage area, land slope, percent impervious, and percent forest. The equations allow the seven parameters of the synthetic streamflow model to be calculated for an ungaged site in the Coastal Plain or Piedmont.

To synthesize a long time series of streamflow for an ungaged site, the parameters are first calculated using the regression equations and drainage basin characteristics from GISHydro2000. A long sequence of streamflow is created by reversing the process used in analysis: generate random numbers using statistical software tools, multiply by the appropriate standard deviation, and add the appropriate mean. The result is a streamflow sequence that possesses realistic interannual variation and day-to-day persistence.

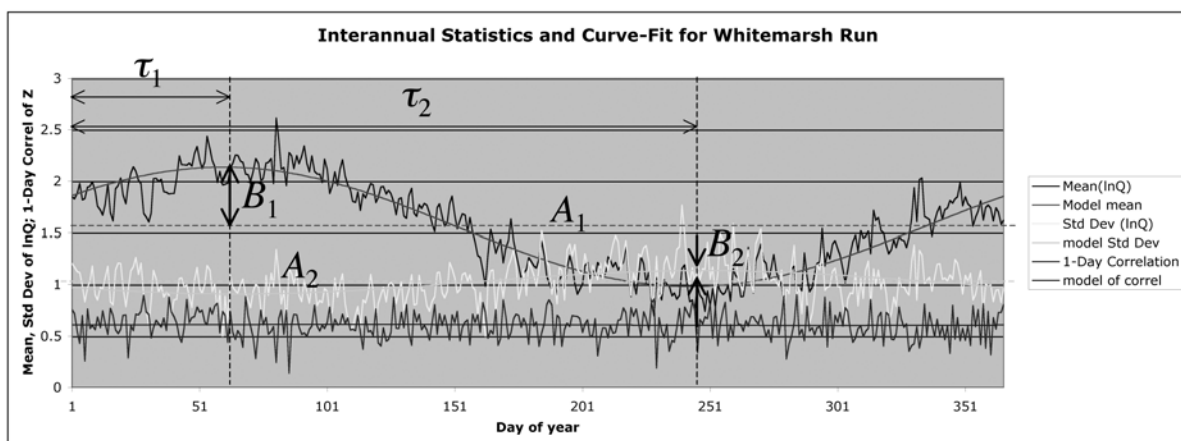


Figure 3.8. Interannual statistics of the natural logarithm of discharge (lnQ) for Whitemarsh Run, showing curve-fit and parameters of the synthetic streamflow model.

The method was tested by comparing synthetic to observed hydrographs for Whitemarsh Run. An example is shown in Figure 3.9. The hydrographs are not an exact match; they are not expected to be, because the synthetic hydrograph is a statistical model, not tied to the physical conditions of any particular year. However, they exhibit similar patterns in terms of the magnitude and duration of the extreme peaks, and the timing and separation of smaller peaks. Figure 3.10 is a magnification of 160 days from the observed and synthetic hydrographs. The synthesized events are similar to the observed events in terms of their steep rising limb and more gradual falling limb.

The synthetic hydrograph method was used to create sequences of daily stream discharge at four of the study sites: MD 7 at White Marsh Run, MD 26 at Monocacy River, MD 28 at Seneca, and MD 355 at Great Seneca. The White Marsh site was collocated with a stream gage; therefore the statistics of observed flow were used to determine the parameters for the streamflow generation routine. At the remaining three sites, a regression equation was applied to determine the parameters. A simulation period of 160 years was selected as having a reasonable probability of including rare, extreme values of discharge. The synthetic discharge hydrographs were created using a Microsoft Excel spreadsheet and stored as text files for input to SRICOS.

Woodrow Wilson Bridge Hydrograph

The synthetic hydrograph method was not applied to the Woodrow Wilson bridge site (I-95/495 over the Potomac), because it was not possible to analyze the Potomac River with GISHydro2000 (the Potomac River basin extends beyond the boundaries of the state of Maryland). The hydrograph used for the Woodrow Wilson Bridge site was based on the USGS Little Falls gage upstream of the bridge. This gage accounts for all but 300 sq. miles of the 11,860 sq. mi. watershed. The 2-, 5-, 10-, 25-, 50-, 100-, and 500-year discharges were adjusted proportionally to the additional contributing area.

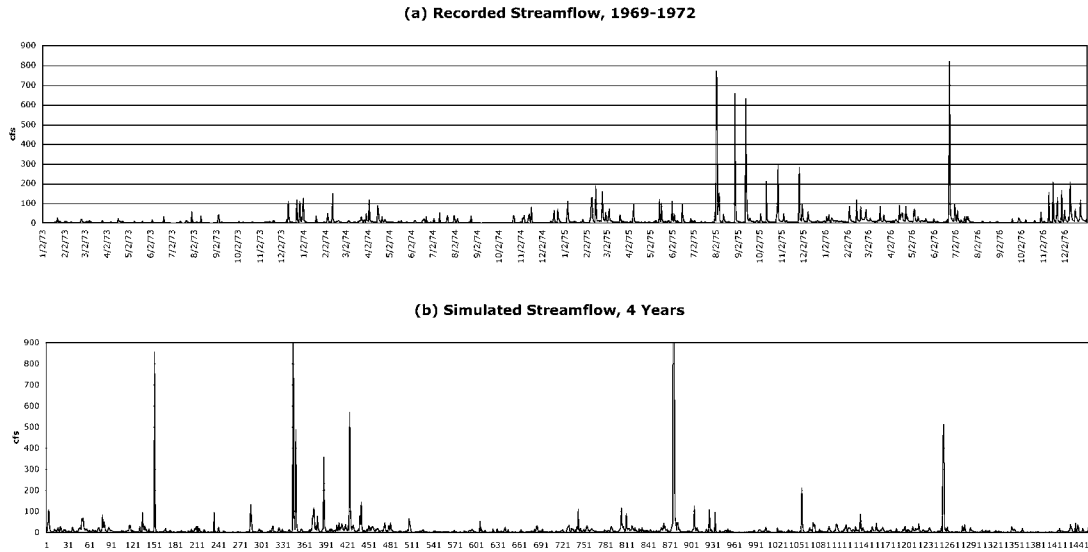


Figure 3.9. Example application of the Simulated Hydrograph method: (a) Recorded streamflow for 1969-1972, (b) Simulated streamflow for a generic four-year period, Whitemarsh Run at White Marsh, Md.

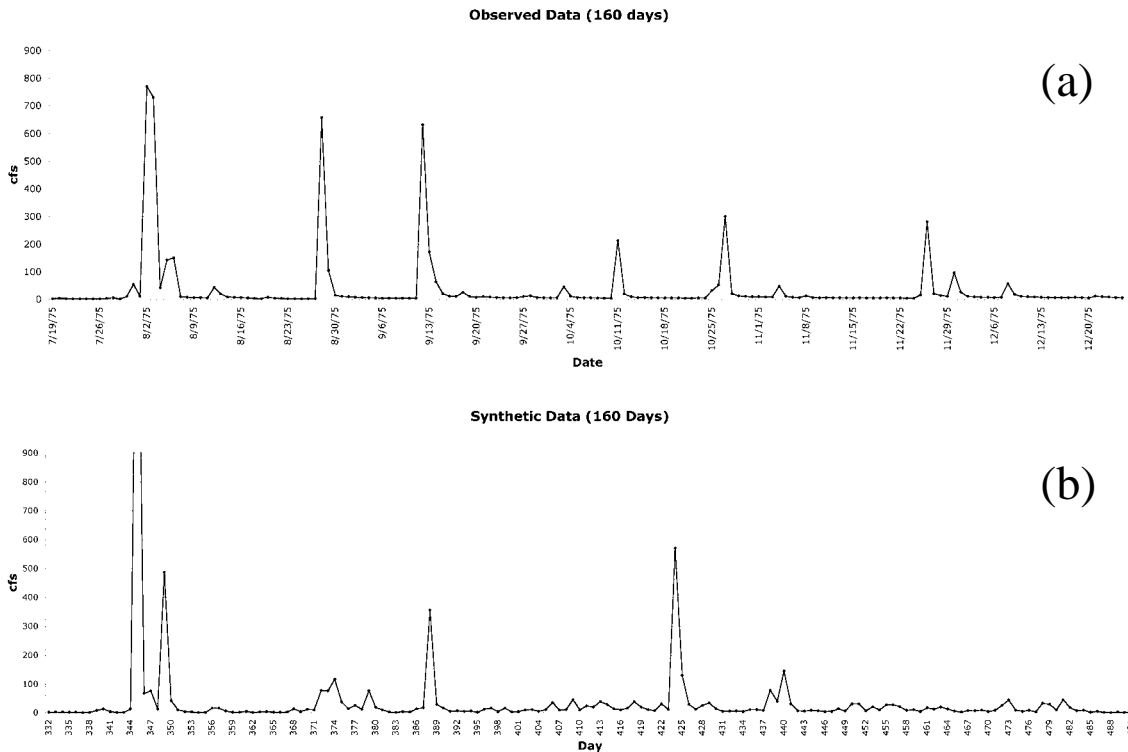


Figure 3.10. Selected 160-day sequences from (a) Observed and (b) Simulated streamflow for Whitemarsh Run at White Marsh.

3.5. Converting Discharge to Velocity Hydrographs.

A model of each bridge site was made in the hydraulic program HEC-RAS (USACE 2002). HEC-RAS is a hydraulic model developed by the U.S. Army Corps of Engineers' Hydrologic Engineering Center and is the most widely used hydraulic program for modeling riverine systems. HEC RAS allows the user to enter surveyed cross sections of the river, structure geometry, friction coefficients, ineffective flow areas, and other variables to obtain water surface elevations, energy elevations and -- most importantly for this project -- flow velocities for given discharges through the bridge cross section. HEC-RAS allows the user to specify up to 45 stream tubes at a given cross section to obtain data on specific areas of concern. Use of this option provided velocity data at the location in front of the piers (whether in the overbank area or the main channel) without the bridge and bridge piers. The reason given for modeling the site without the bridge in place is "removal of the piers is necessary because the velocity used for the pier scour calculations is the mean depth velocity at the pier location if the pier were not there." (Briaud et al. 2003)

A table was made of the velocity for a given discharge at the selected pier. Varying discharges were run through the hydraulic program to provide a curve of discharge vs. velocity and velocity vs. water depth in the overbank area where the pier is located. These tables are required input to the SRICOS program. The tables developed for the Maryland study differ from the original SRICOS method in that the piers in the Texas study were in the river channel and therefore had higher velocities associated with the discharges. The tables were entered into the water data window of the SRICOS program.

3.5. Predicting Bridge Pier Scour at Maryland Sites with SRICOS

Once the velocity hydrograph and the shear stress vs. erosion curve are developed, the SRICOS program can be run. The program uses the following steps to calculate the maximum scour depth at a complex pier as outlined in the SRICOS manual.

The SRICOS program was originally developed to predict the scour depth versus

time for circular piers in deep water at a constant velocity and a uniform soil. This equation was modified for other conditions and geometries, with correction factors to account for shallow water depth, effect of rectangular shapes, angle of attack, and pier spacing (Briaud et al. 2003). However, the method does not account for the effect of exposed footings at this time. SRICOS requires an erosion rate versus the hydraulic shear stress curve, obtained from the EFA tests. The maximum hydraulic shear stress (τ_{\max}) around the pier is calculated first. The initial erosion rate corresponding to τ_{\max} is read from the erosion rate curve that was developed empirically. The maximum shear stress for a given velocity is calculated as:

$$\tau_{\max}(\text{pier}) = k_w k_{sh} k_{sp} k_{\alpha} \left[0.094 \rho V^2 \left(\frac{1}{\log \text{Re}} - 0.1 \right) \right] \quad (3-2)$$

where

$\tau_{\max}(\text{pier})$ is the maximum shear stress around the pier

ρ is the mass density of water

Re is the Reynolds number equal to VB/ν

V is the depth-mean velocity at the location of the pier if the bridge was not there

B is the pier diameter or pier width

ν (Greek “nu”) is the kinematic viscosity of water

The k factors take shallow water depth, pier shape, pier spacing and attack angle (α) into account respectively, and are obtained from look-up tables in the SRICOS manual.

The next step is to calculate the maximum scour depth, z_{\max} , corresponding to a particular velocity:

$$z_{\max}(\text{pier}) = K_w K_{sp} K_{sh} (0.18 \text{Re}^{0.635}) \quad (3-3)$$

where $z_{\max}(\text{pier})$ is the maximum depth of pier scour in millimeters;

Re is the Reynolds number equal to VB'/ν as described earlier, V (ft/s) being the mean depth velocity at the location of the pier if the bridge was not there, and

B' is the projected width of the pier, taking account of attack angle.

K_w is the shallow water factor, computed as follows:

$$\begin{aligned} \text{For } H/B \leq 1.6 \quad K_w &= 0.85(H/B)^{0.034} \\ \text{For } H/B > 1.6 \quad K_w &= 1 \end{aligned} \quad (3-4)$$

where

H = water depth,

B = pier width

K_{sh} is the shape factor, computed as follows

$$K_{sh} = \frac{B_1}{B_1 - nB} \quad (3-5)$$

where

n = piers of diameter B in row; and

K_{sp} is the spacing factor.

Finally, the erosion vs. time curve is constructed. The SRICOS program computes the scour depth corresponding to a particular flood from this curve. The shape of the scour depth versus time curve is defined as:

$$z = \frac{t}{1/\dot{z}_i + t/z_{\max}} \quad (3-6)$$

where \dot{z}_i is the initial slope of the scour versus time curve (found from the EFA results), and t is the duration of the flood event of velocity V , in hours.

This procedure describes the evolution of scour depth associated with a single velocity. However rivers have varying discharges and velocities over time. The SRICOS researchers accounts for time-varying velocity by analyzing the flood in a series of time segments. The velocity hydrograph is treated as a series of partial flood events of equal duration (24 hours for the daily hydrograph). Two velocities are handled by assigning the velocities as V_1 and V_2 and the time of the events as t_1 and t_2 . Each velocity has a

corresponding maximum scour depth, computed from Eq. 3-3. The scour depth versus time curve for flood 1 is computed as:

$$z_1 = \frac{t_1}{1/\dot{z}_{i1} + t/z_{\max 1}} \quad (3-7)$$

And for flood 2 as:

$$z_2 = \frac{t_2}{1/\dot{z}_{i2} + t/z_{\max 2}} \quad (3-8)$$

If V_2 is greater than V_1 , flood 1 creates a scour depth z_1 that would have been created in a shorter time, t_e , by flood 2. This shorter time can be found by the equation:

$$t_e = \frac{t_1}{\dot{z}_{i2}/\dot{z}_{i1} + t_1\dot{z}_{i2}(1/z_{\max 1} - 1/z_{\max 2})} \quad (3-9)$$

Flood 2 starts at a scour depth of z_1 , which is equivalent to having flood 2 for time t_e to achieve the same scour depth. The program advances through a sequence of 24-hour flood velocities by considering a new “flood 2” and a new t_e at each new velocity. The output of the program is the scour depth over the entire duration of the hydrograph.

In the case of multi-layered soils, when the scour depth enters a new soil layer, the computations follow the same process, now using the new layer’s erosion rate versus shear stress curve and starting at the previous flood’s final scour depth. The SRICOS code steps are outlined in Briaud (2003).

SRICOS allows the user to insert a 100- and/or 500-year storm into the hydrograph at proscribed intervals. Since four of the synthetic hydrographs used in the SRICOS program did not show a 100-year storm, the SRICOS option of inserting the 100-year storm was used in all cases. The synthetic hydrograph for MD 7 over Whitmarsh Run contained a discharge larger than the 500-year storm. However, due to the geometry of the structure and the high tailwater, the 500-year storm had bridge

velocities that were smaller than the 100-year discharge; therefore, the 100-year storm was inserted into the hydrograph.

The SRICOS program converts the discharge hydrograph into a velocity hydrograph and provides a table of velocity, maximum scour depth, and accumulated scour depth for all given discharges, with a final scour depth reported for the last discharge entry on the hydrograph.

For comparison purposes the HEC-18 pier scour depth (FHWA 2001, described in Section 2.2) was also calculated. HEC-18 has become the standard method used by engineers to estimate maximum design pier scour. The equation, however, is designed for cohesionless soils and is independent of time. It is widely regarded as being a conservative estimate of scour in cohesive soils.

4. Findings

This chapter presents the findings of the study. In Sections 4.1 through 4.4, the order of presentation is the same as the description of methods in Chapter 3: analysis of soil characteristics, EFA tests of erosion rate, discharge hydrograph development, converting discharge to velocity hydrographs, and predicting bridge pier scour using SRICOS. Following these results, an additional three sections describe investigations that were undertaken in the course of the study as questions arose that had not been considered in the original study design: critical velocity determination, sensitivity of SRICOS calculations to discharge order, and the implications of inserting instantaneous peak flows into a daily-discharge hydrograph.

4.1. Soil Characteristics and EFA Data

Shelby-tube boring samples were collected from each of the five study sites. The soil characteristics of each sample are listed in Table 4-1. The Erosion Function Tables for each tested Shelby tube are tabulated in Appendix A and are graphed as erosion rate versus shear stress in Figures 4.1 -4.10.

Three usable Shelby tube samples were collected at the White Marsh Run site, all at a depth between 1' – 3'. These sample tubes were bored in the vicinity of the proposed bridge pier in the overbank area. The three tubes were all classified under the USCS soil classification system as sandy lean clay with D_{50} of 0.0234mm, 0.0530mm and 0.389mm respectively. The Atterberg Limits were also quite similar, as can be seen in Table 4.1 and the plasticity chart shows soils of inorganic clays of low plasticity.

Two Shelby tubes were recovered from the Monocacy River site, which were classified by USCS as lean clay with sand. Again the Atterberg Limits of the two samples are quite similar and represent inorganic clays of medium plasticity on the plasticity chart while the D_{50} of the two samples are 0.0178mm and 0.0087mm.

Three Shelby tubes were collected at the Seneca Creek site and four analyses were performed. These samples had different soil classifications assigned to them. The first tube, recovered at a depth of 5' to 7', was classified as silt with a D_{50} of 0.0114mm. The second

Table 4.1. Comparison Table of Shelby-Tube Soil Samples

Site	Boring	Liquid Limit, %	Plasticity Index, %	D50(mm)	% Gravel	%Sand	% Silt	% Clay	% Passing 200 Sieve	Unified Soil Type
MD 28	B-Tube 1, 5'-7'	35	13	0.0178	7.6	15.4	51.1	25.9	77	CL-lean clay w/ sand
	Tube 2, 7'-8.5'	39	11	0.0114	0	4.2	67.8	28	95.8	ML - silt
	B-3A 5'-7' 1st analysis	N/P	N/P	0.0328	0	29.8	50.3	19.9	70.2	ML-silt w/ sand
	5'-7' 2nd analysis	30	8	0.0358	0	26.5	55.3	18.2	73.5	CL-lean clay w/ sand
MD 26	B-1 Tube 1, 4'-8'	38	14	0.0074	2.8	5.7	52.9	38.6	91.5	CL-lean clay
	Tube 2, 6'-8'	36	13	0.0087	0	19.2	43.7	37.1	90.7	CL-lean clay w/ sand
MD 355	B-2 Tube 1, 2'-4'	28	21	0.0243	6.8	17.1	55.5	20.6	76.1	CL-sandy lean clay
	Tube 2, 6.5'-8.5'	29	8	0.0442	5.9	30.3	40.8	23	63.8	CL-sandy lean clay
MD 7	B-3 Tube 1, 1'-3'	26	8	0.0234	3.7	35.1	32.3	28.9	61.2	CL-sandy lean clay
	B-2A Tube 2, 1'-3'	24	8	0.053	8.8	37	27	25.2	52.2	CL-sandy lean clay
	B-2 Tube 3, 1'-3'	25	9	0.0389	6.5	39	27.3	27.2	54.5	CL-sandy lean clay
VWV Br.	B-8 72'-73'	76	40		16.3	1.2	7.1	75.4	82.5	day
	B-3 58'-60'	N/P	N/P	0.308	2.8	85	7	5.2	12.2	sand

tube, recovered at a depth of 7' to 8.5' in the same boring hole as tube 1, was classified as lean clay with sand, with a D_{50} of 0.0178. The third tube, recovered at a depth of between 5' and 7', was classified as silt with sand and had a D_{50} of 0.0328mm in the first analysis, which represented the first 12 inches of soil recovered. During the EFA testing of the next 12 inches of tube 3, it became apparent that another type of soil layer had been uncovered. This soil was analyzed separately for soil characteristics and classified as lean clay with sand; it had a D_{50} of 0.0358mm.

The two tubes recovered from the Great Seneca Creek site over MD 355 were collected from the same boring hole at 2' to 4' for tube 1 and 6.5' to 8.5' for tube 2. The soil of tube 1 was classified as lean clay with sand and had a D_{50} of 0.0243mm. The soil of tube 2 was classified as sandy lean clay with a D_{50} of 0.0442mm.

Finally, because the Woodrow Wilson Bridge is one of the busiest interstate bridges in the country, retrieval of Shelby tubes from the bridge was impossible. In addition, the cost of using a river barge to retrieve the tubes was prohibitive. After careful analysis of the known soil layers under the bridge, the same soil layers were located by MSHA geotechnical engineers on the Maryland shore at a depth of 58'-60' for tube 1 and a depth of 72' to 73' for tube 2. Tube 1 had a D_{50} of 0.308 and a soil classification of silty sand. Tube 2 had a D_{50} that was too small to ascertain. 81.7% of the soil was finer than #270 sieve; however the D_{85} was 2.24mm and a soil classification of clay with 84% of the soil being clay, 14% silt and 2% sand.

The erosion rate curves for each EFA tested site were developed. These results are graphed in Figures 4.1 through 4.10. They are input in tabular form to the SRICOS program; the tables corresponding to Figs. 4.1. through 4.10 are included as an Appendix to this report. The EFA measures the velocity in m/s and erosion rate in mm/hr. The equation for shear stress ($\tau = 1/8 f\rho V^2$) was used to obtain the erosion rate vs. shear stress curves. The shear stress was then converted to English units (lbs/ft²), as were all other units except for the erosion, which SRICOS requires to be entered in metric units, for ease of use with previous studies.

The Woodrow Wilson Bridge Shelby tubes presented some problems. The first Shelby tube taken at a depth of 58'-60' was found to have dent in the middle of the tube. This prevented the EFA piston from pushing the sample and required stopping the tests

before a full EFA test of the material could be performed. The second Shelby tube, taken at a depth of 72', contained very stiff clay that was too stiff for the motor of the piston to push. This test was also terminated and no results were possible.

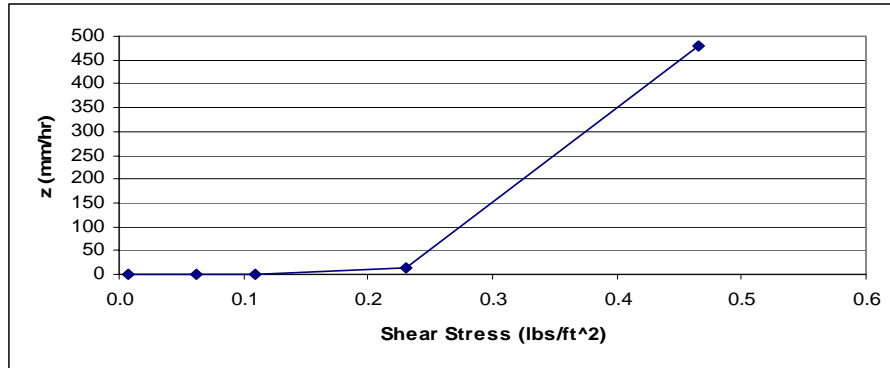


Figure 4.1. Erosion Rate Curve, MD 26 over Monocacy River, Tube 1

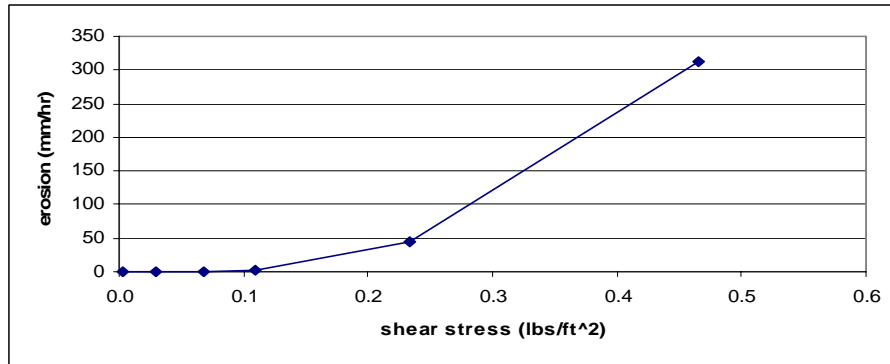


Figure 4.2. Erosion Rate Curve, MD 26 over Monocacy River, Tube 2

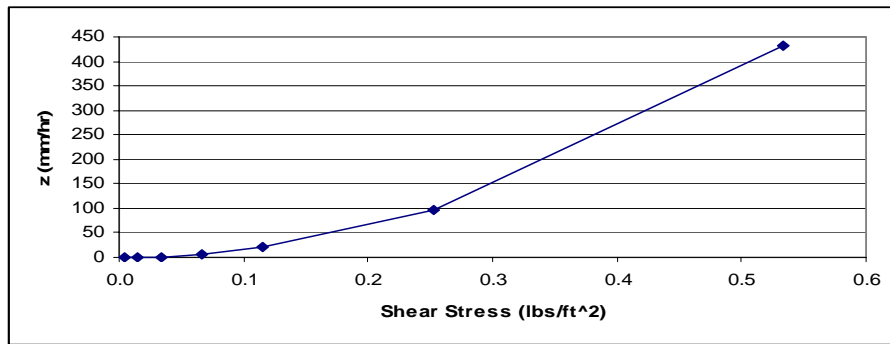


Figure 4.3. Erosion Rate Curve, MD 355 over Great Seneca Creek, Tube 1, 2'-4'

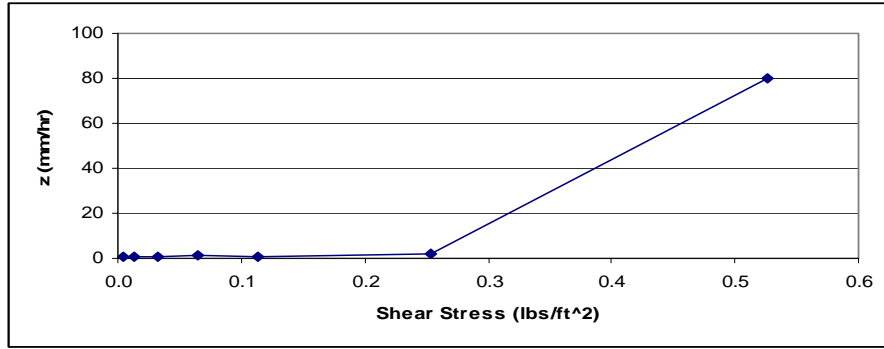


Figure 4.4. Erosion Rate Curve, MD 355 over Great Seneca Creek, Tube 2, 6'-8'

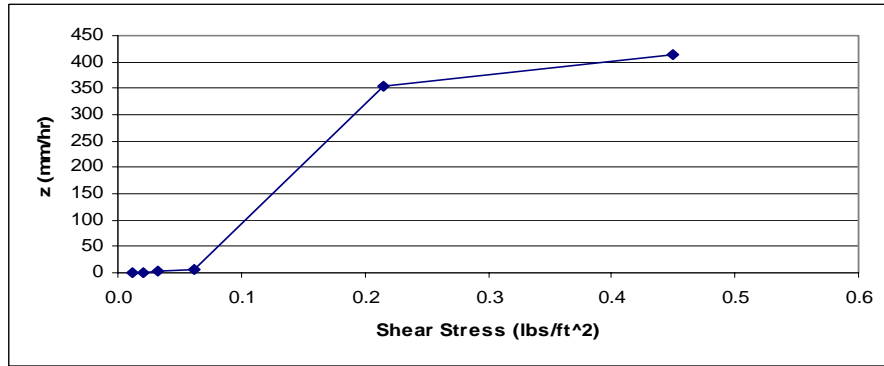


Figure 4.5. Erosion Rate Curve, MD 28 over Seneca Creek, Tube B-3A, 5'-7'



Figure 4.6. Erosion Rate Curve, MD 28 over Seneca Creek, Tube B-3, 5'-7'

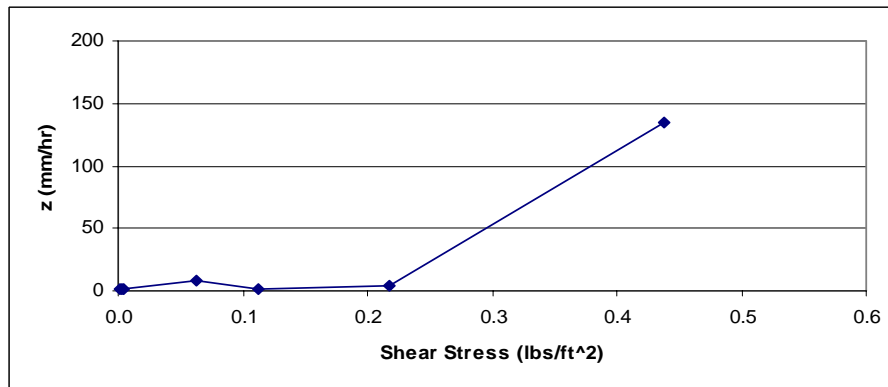


Figure 4.7. Erosion Rate Curve, MD 28 over Seneca Creek, Tube B-3, 7'-8.5'

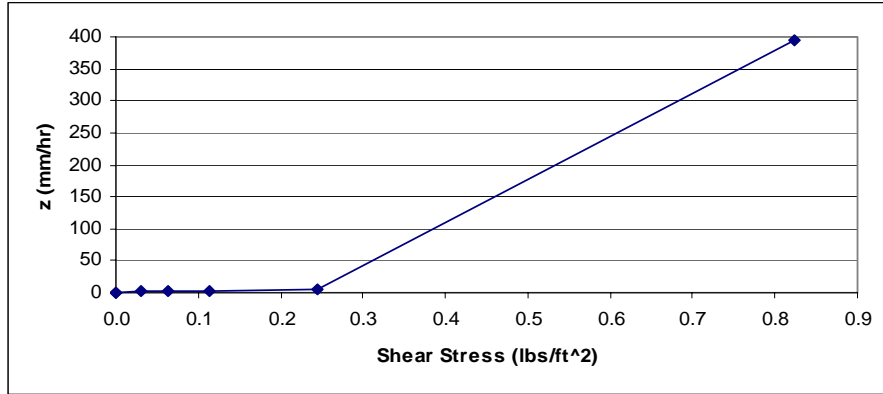


Figure 4.8. Erosion Rate Curve, MD 7 over White Marsh Run, Tube 1, 1'-3'

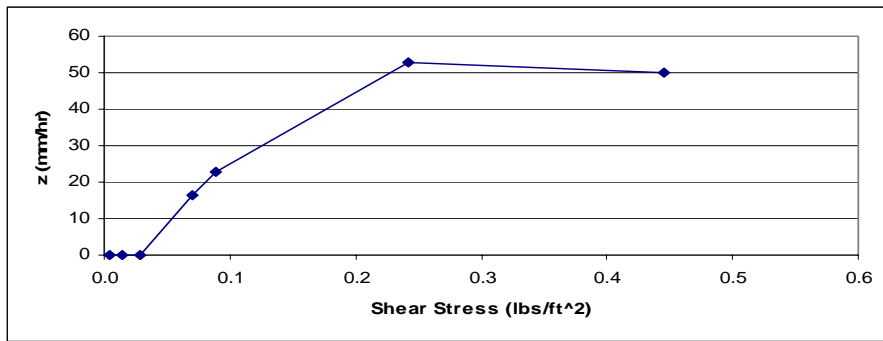


Figure 4.9. Erosion Rate Curve, MD 7 over White Marsh Run, Tube 2, 1'-3'

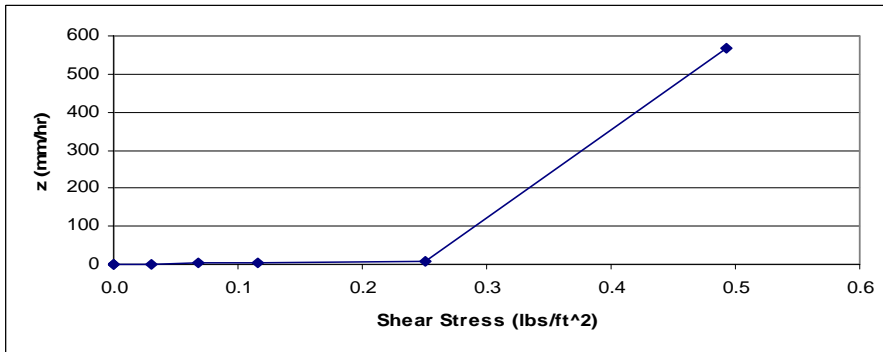


Figure 4.10. Erosion Rate Curve, MD 7 over White Marsh Run, Tube 3, 1'-3'

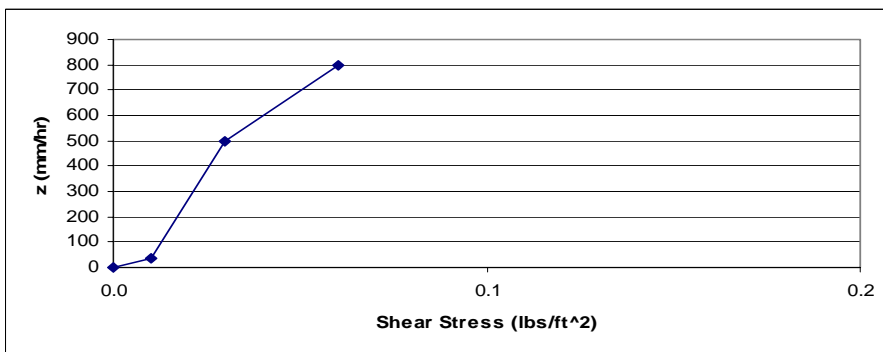


Figure 4.11. Erosion Rate Curve, MD 495 over Potomac River, Tube 58'-60'

4.2 Synthetic Streamflow for Study Sites

The method developed in this study (summarized in Section 3.4 and described in the Appendix) was used to create several 160-year sequences of synthetic daily stream discharge at four of the study sites: MD 7 at White Marsh Run, MD 26 at Monocacy River, MD 28 at Seneca, and MD 355 at Great Seneca. As explained in Section 3.3, a modified 80-year observed hydrograph was used for I-95/495 (Woodrow Wilson Bridget) at Potomac River.

The White Marsh site was collocated with a stream gage; therefore the statistics of observed flow were used to determine the parameters for the streamflow generation routine. At the remaining three sites, the Piedmont regression equations, determined as described in Section 3.3, were applied to estimate the parameters of the synthetic hydrograph model. One site, MD 26 over the Monocacy River, is actually located in the Great Valley geographic province; however, the Piedmont equations were used for this site as well. The sample of gaged basins from the Great Valley province in Maryland was too small for regression analysis.

The predictor equations for the seven model parameters in the Piedmont region are given below.

$$\begin{aligned}
 A_1 &= 1.031649 * \ln(\text{Drain_Area}) - 0.229384 * (\%_Storage) \\
 &\quad - 0.015375 * (\%_Imperv) + 2.139343 * (224_Prec) - 6.484614 \\
 B_1 &= -1.568516 * (224_Prec) - 3.034949 * (\text{Slope_Land}) \\
 &\quad + 0.002229 * (\text{Flow_Path}) + 5.360096 \\
 \tau_1 &= 429.4137 * (\text{Slope_Land}) - 0.445061 * (\%_Forest) \\
 &\quad + 3.358239 * (\%_Storage) - 1.51006 * \ln(\text{Drain_Area}) + 56.58506 \\
 A_2 &= 0.271254 * (\%_Storage) + 0.008082 * (\%_Imperv) \\
 &\quad - 0.003219 * (\%_BSoils) + 0.841717 \\
 B_2 &= 0.002243 * (\%_Urban) - 0.005852 * (\text{Aver_CN}) \\
 &\quad - 0.380106 * (224_Prec) - 0.001668 * (\%_ASoils) + 1.586495 \\
 \tau_2 &= -0.359175 * (\%_BSoils) - 135.0956 * (224_Prec) \\
 &\quad - 0.700418 * (\%_Forest) - 0.262481 * (\%_Urban) + 711.6274 \\
 A_3 &= -0.00642 * (\%_Imperv) + 0.049798 * (\%_Storage) \\
 &\quad + 0.001325 * (\%_Forest) + 0.788938
 \end{aligned} \tag{4-1}$$

where

$\ln(\text{Drain_Area})$ = natural logarithm of basin drainage area
 $\%_Storage$ = fraction of area (as a percent) contributing hydrologic storage
 $\%_Imperv$ = fraction of area (as a percent) that is impervious to infiltration
 224_Prec = 2-year, 24-hour precipitation
 $Slope_Land$ = average slope of the land surface
 $Flow_Path$ = length of longest travel path for water in the basin
 $\%_ASoils, \%_BSoils$ = the fraction of area (as a percent) consisting of, respectively, type “A” and type “B” soils
 $\%_Urban, \%_Forest$ = fraction of area (as a percent) identified as, respectively, urban and forested land use

The model parameters describing the annual cycle of average flow, the annual cycle of variability in flow (standard deviation) and the one-day lag correlation of the standardized flows for each site are plotted in Fig. 4.12. This figure is included to demonstrate that the analyzed sites lie within the range of properties used in calibrating the regression model. The resulting annual patterns of average flow, standard deviation of flow, and day-to-day persistence are plotted in Fig. 4.13.

Synthetic 160-year daily discharge hydrographs were created using a spreadsheet implementation of the simulation method described in Section 3.3. These discharge hydrographs were then supplied as input to the SRICOS program.

One feature of SRICOS is that it also allows the user to supply estimates of the 100- and 500-year discharge at the study site. The program adds these rare, extreme discharge values to the input hydrograph to ensure that the major scour-inducing events are included in the hydrograph. This step is considered necessary because, for example, the probability of sampling the 500-year discharge in a simulation of 160 years is only about 27% -- assuming that the simulation is built on the correct statistical distribution of discharge.

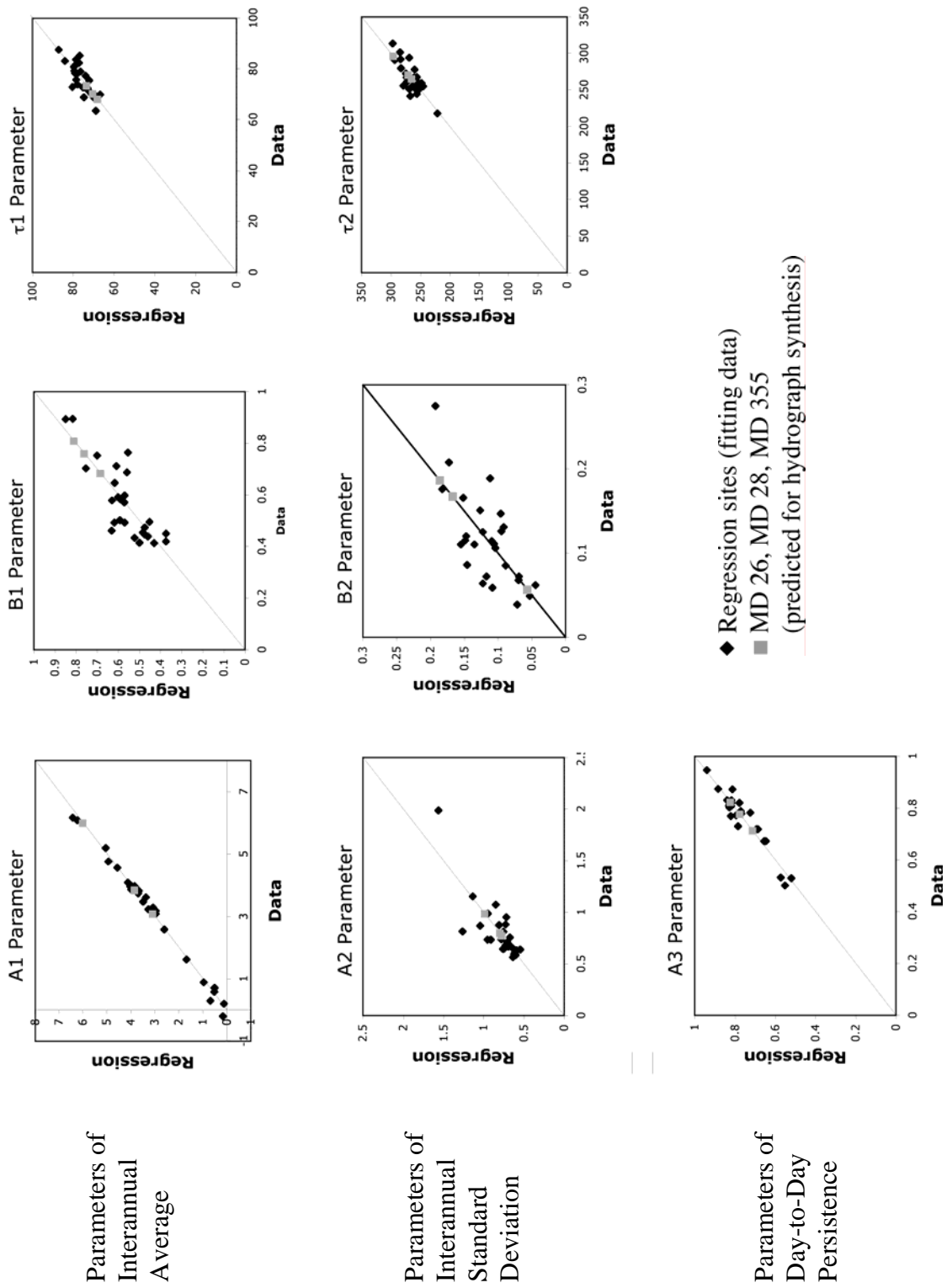


Figure 4.12. Parameters of the synthetic streamflow model, showing study sites in the range of calibration.

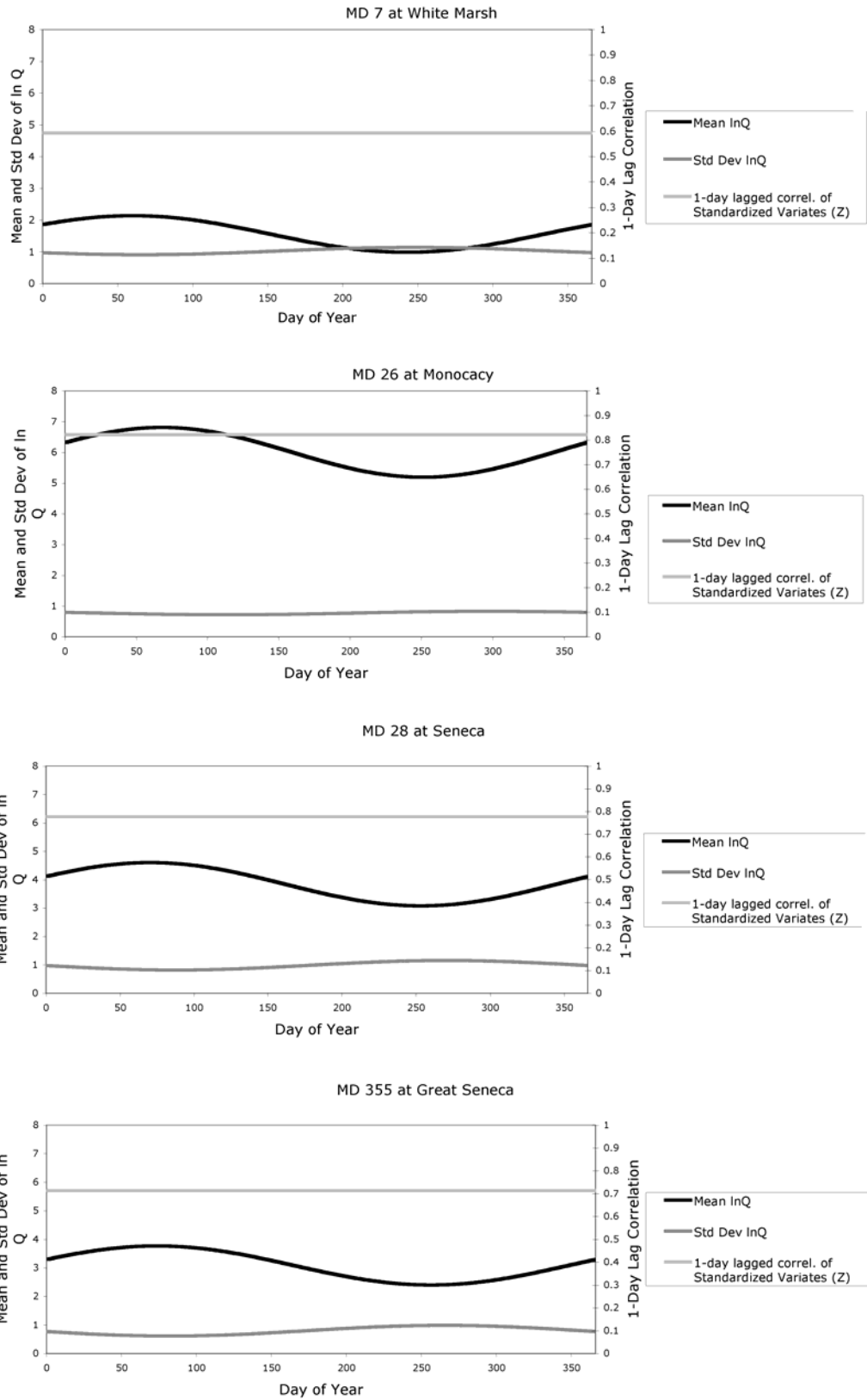


Figure 4.13. Synthetic hydrograph model: annual cycle of mean, standard deviation, and day-to-day persistence (correlation) of $\ln(Q)$ for four study sites.

An analysis tool of GISHydro2000 was used to calculate 100- and 500-year instantaneous peak discharges at the study sites, under conditions of ultimate development, as dictated by MSHA’s design philosophy. Of the synthetic hydrographs generated, only the White Marsh Run site contained a daily discharge that was greater than the 500-year storm flow. None of the four sites had a daily discharge equal to the 100-year discharge. In addition to the sampling issue discussed above, there are two other reasons why the synthetic hydrographs did not include these extreme values of discharge: First, the 100- and 500-year values predicted by the GISHydro2000 tool are instantaneous peak flows, whereas the synthetic hydrograph method produces 24-hour (daily average) flows; and second, the parameters for the study sites were estimated from the regression equations based on current, rather than ultimate-development, conditions. These issues are discussed later in this report. In order to ensure that the worse-case scenario was included in the simulation, and for HEC-18 comparison purposes, the 100-year flood event was inserted manually into the SRICOS program at all four sites. The 100-year instantaneous discharges, as calculated in GISHydro2000, are listed in Table 4.2.

As explained in Section 3.4, the Potomac River hydrograph was a modified USGS daily-discharge hydrograph of 80 years duration. Estimates of the 100-year and 500-year peak flows are 480,000 cfs and 575,000 cfs respectively (FHWA, 2000). The Potomac River hydrograph included a daily discharge of 465,000 cfs that was quite close to the 100-year instantaneous peak event of 480,000 cfs; therefore, no extra flood events were inserted into SRICOS for this site.

Table 4.2. Instantaneous 100-Year Peak Flow (Ultimate Development)

Site	100-year Peak Flow* (cfs)
White Marsh Run	6300
Monocacy River	81600
Great Seneca Creek	17400
Seneca Creek	30470

*Estimated using GISHydro2000

4.3. Hydraulic Models

All five selected sites had previously undergone extensive hydraulic analysis in preparation for replacement or added bridges. The SRICOS method suggests using only a few cross sections depicting the stream topography immediately upstream and downstream of the bridge as well as the bridge crossing itself; however, MSHA personnel had developed hydraulic models that included a number of stream cross-sections 1000-2000 ft. upstream and downstream of each bridge. This more extensive characterization of channel geometry generates more accurate model estimates of flow velocities and water surface elevations in the vicinity of the bridge. The HEC-RAS models used for this study were based on the previous hydraulic models prepared for the new bridges.

Two of the models, MD 26 over the Monocacy River and MD 28 over Seneca Creek, were originally developed in HEC-2 and were converted into HEC-RAS. In accordance with the SRICOS method (Briaud et al. 1999), the bridge geometry was removed from all the models but the roads, road embankments, and ineffective areas were left intact. Cross sections were placed at the toe of slope to provide velocity readings upstream of the piers.

The discharges run through the models included the 2-, 10-, 25-, 50-, 100-, and 500-year design storms. Unlike the Texas bridge piers studied in previous SRICOS reports (Briaud et al. 1999; 2001a,b; 2003), where the piers are found in the main channel, Maryland bridge piers are placed outside the main channel in an effort to minimize stream degradation in the vicinity of the bridge. With the use of the stream tube option in HEC-RAS, it was possible to ascertain the flow velocity immediately upstream of the pier. The velocities and water depths of this study reflect flows at the pier locations, whether they are in the overbank or in the main channel. For certain configurations, the velocity at the pier may be much lower than in the main channel, even at large overall stream discharge values.

The HEC-RAS analysis produced tables of velocity and water depth at the pier location for the specified discharges. These tables are required as input to the SRICOS method. Cross sections at the pier locations and the discharge-velocity tables developed in HEC-RAS are provided in an Appendix to this report.

4.4. Bridge Pier Scour Estimates

The Erosion Function data (Section 4.1), the 160-year daily discharge hydrographs (Section 4.2), and the discharge-velocity and discharge-depth rating curves produced using HEC-RAS (Section 4.3) provided the necessary input to predict scour at the study sites using the SRICOS program. The SRICOS option to insert the 100-year storm into the hydrograph was used for all sites but the Woodrow Wilson Bridge; SRICOS places the inserted discharge midway through the hydrograph. The pier erosion results are presented graphically as Figures 4-14 through 4-18. The time axis of each Figure is in years, from 0 to 160; it should be noted that 58,440 daily values are represented by each scour depth plot.

The Whitmarsh Run hydrograph included a daily average discharge greater than the predicted instantaneous 500-year discharge. But that extremely high discharge overtopped the bridge and had a lower velocity at the bridge pier location than the inserted 100-year discharge. As a result, Figure 4.14 shows that the 100-year discharge (inserted midway through the hydrograph, at Year 80) caused much of the predicted pier scour for the MD 7 Bridge over Whitmarsh Run. More than half of the total scour (about 1.5 ft) occurred during the first 365 days of simulation, between years 0 and 1; due to the graphical scale (58,440 days plotted as 160 years), the scour depth history appears to start from 1.5 feet at time 0, but in fact it rises from 0 to 1.5 in a short time.

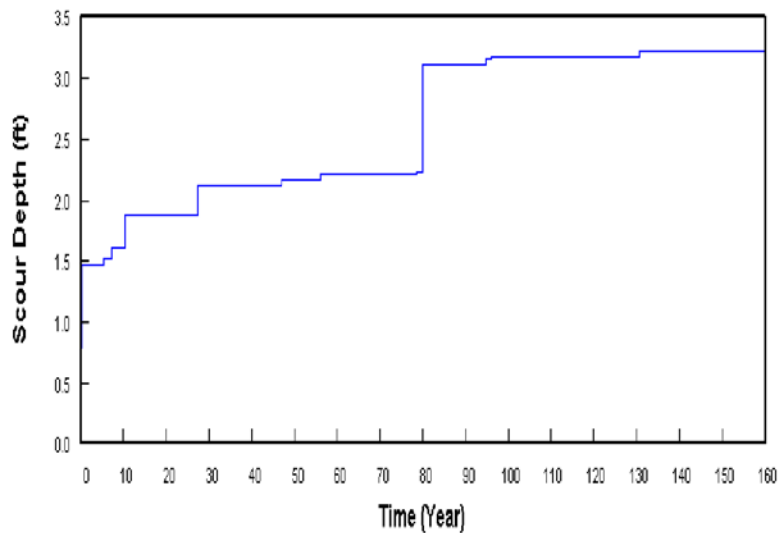


Figure 4.14. SRICOS predicted pier scour, MD 7 over Whitmarsh Run.

The pier of the MD 26 Bridge over the Monocacy River sits out of the daily base flow but it is subjected to larger flows. Figure 4.15 shows approximately 3 feet of predicted scour that jumps to approximately 8 feet of scour produced by the 100-year inserted discharge at Year 80. Again, rapid scouring during Year 1 leads to an apparent value of almost 2 feet at the origin, but this scour actually occurs during the first year (365 days) of simulation.

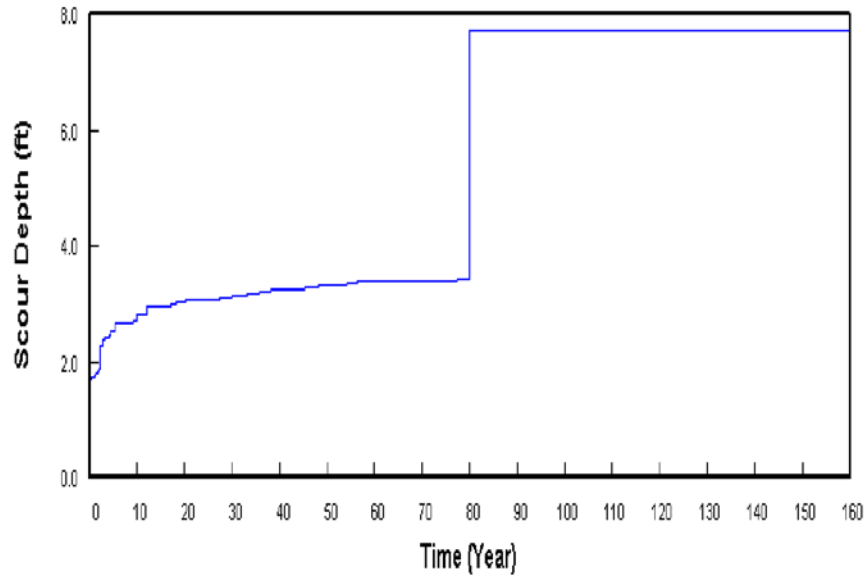


Figure 4.15. SRICOS predicted pier scour, MD 26 over Monocacy River.

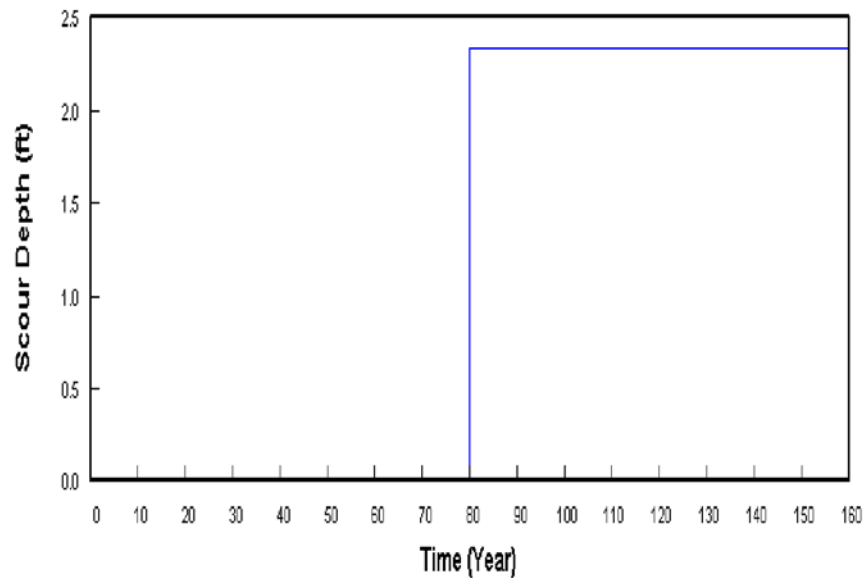


Figure 4.16. SRICOS predicted pier scour, MD 355 over Great Seneca Creek.

Scour at the Great Seneca Creek bridge pier (Fig. 4.16) also shows that the 100-year inserted storm was the cause of all scour at this bridge. For MD 28 over Seneca Creek (Fig. 4.17), even the inserted 100-year discharge produces only 0.2 ft of scour; a very small scour depth due to the large bridge length (more than 500 ft) and the low flow velocities in the overbank area. For the Woodrow Wilson Bridge, I-95/495 over the Potomac River, where the adjusted USGS 80-year hydrograph was used without insertion of additional extreme flows,

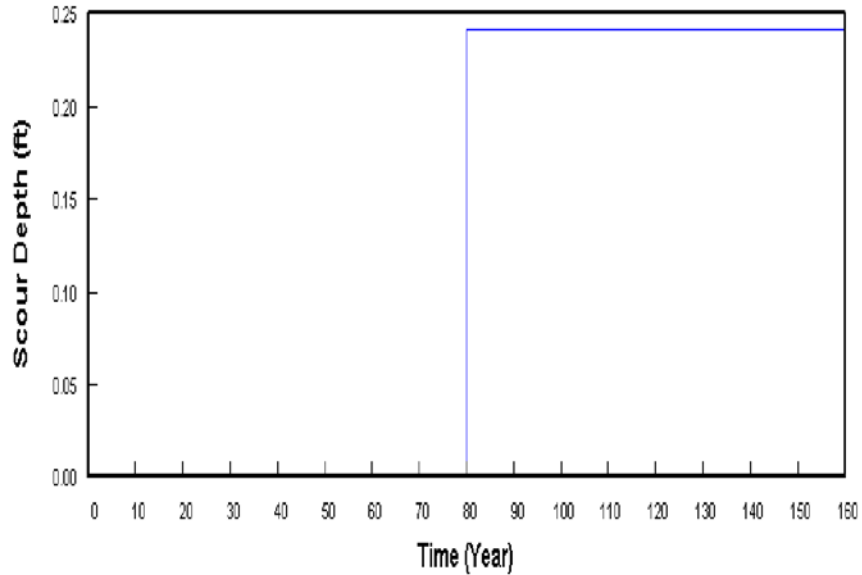


Figure 4.17. SRICOS predicted pier scour, MD 28 at Seneca Creek.

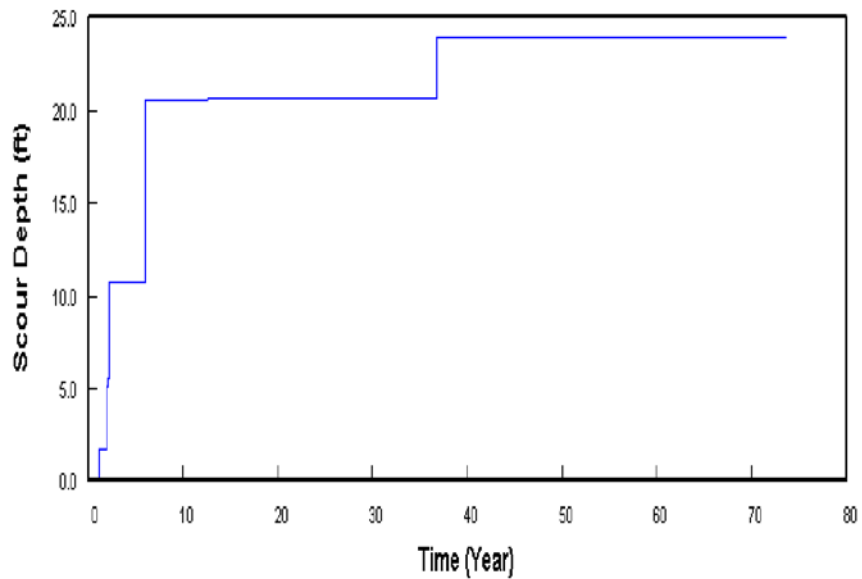


Figure 4.18. SRICOS predicted pier scour, I-95/495 at Potomac River (Woodrow Wilson Bridge).

Table 4.3. Comparison of scour depths predicted by SRICOS and HEC-18

Site	SRICOS Scour (ft)	HEC-18 Scour (ft)
MD 28 over Seneca Creek	0.2	8.4
MD 355 over Great Seneca Creek	2.3	4
MD 26 over Monocacy River	7.7	12.4
MD 7 over White Marsh Run	3.2	5.4
I-95/495 over Potomac River (Woodrow Wilson Br.)	26.5 (incomplete)	30-46

several large events other than the 100-year discharge all contribute to the pier scour (Figure 4.18).

Pier scour predictions were computed for each site using the standard HEC-18 method, as described in Section 2.2. Results are summarized in Table 4-3. As expected, the HEC-18 predictions, which assume non-cohesive soil, are higher than the SRICOS predictions. All HEC-18 calculations relied upon the data generated by the HEC-RAS hydraulic models with the proposed bridges in place, following MSHA standard design procedure.

Although the SRICOS scour depths are less than the HEC-18 scour depths (Table 4.3) it is MSHA policy to predict a minimum of 5 feet of scour at bridge structures. Three of the five selected sites have SRICOS scour depths that are less than five feet. Consequently these scour depths would have been increased to the minimum five feet, notwithstanding the EFA/SRICOS calculations at these sites. The two predicted scour depths for the Woodrow Wilson Bridge site were comparable, although the SRICOS scour depths are not complete due to mechanical problems encountered with the soil samples.

4.5. Critical Velocity Tests

Briaud et al. (1999, 2001a,b) determine the critical velocity and critical shear stress as those that correspond to the shear and velocity that produce 1mm of erosion. Since this

method of determining the critical velocity may bracket the true critical velocity, another test was conducted on 4 of the 5 samples. This new experiment was performed to ascertain the actual critical velocity of the soil. The test used the same Shelby tube soil samples as above and the sample was prepared in the same manner; i.e. the Shelby tube was placed on the EFA piston and the sample was trimmed flush with the top of the tube. However prior to placing the tube flush to the flume bottom, a waterproof colored marker was used to place 9-10 dots on the top of the centerline of the soil sample, 5mm from the downstream end of the tube. The dots were placed in a straight line that was approximately 10mm in length. The area for the placement of the dots was chosen to avoid the small micro-eddies produced by the tube rim. The sample was placed flush to the bottom of the flume as before but this time the sample was not pushed into the flow. The initial velocity was kept constant and slow (approximately 0.5m/s). If no erosion of the dots occurred within one minute the velocity was increased and the dots were observed again. If after 1 minute no change in the dots was observed, the velocity was increased in the same manner until movement was observed. When the dots began to fade, the velocity was kept constant and the time to fully erode the dots was recorded along with the velocity. This procedure was repeated 8 to 9 times with velocities that bracketed the initial velocity where movement was observed to obtain a velocity curve from which the critical velocity could be determined. It was believed that this method would give a more accurate threshold shear for very small D_{50} material that could help extend and refine Neill's curves (Neill 1973), one method of estimating critical velocities in fine materials such as sands and silts. Neill showed that small bed-material grain size eroded at small competent (critical) velocities and that large bed-material grain size eroded at high competent (critical) velocities in a straight-line relationship. Neill believed that there was some influence of fine materials on the resistance of soil for a D_{50} size below 0.3mm (fine sand), which is why his curves stop at that particle size.

In Figure 4.19, results of the critical velocity tests are plotted on Neill's chart for critical velocity of sandy soils as a function of water depth, velocity and flow depth. (TAC, 2001) The dots on the left of the chart represent the critical velocity (competent velocity on chart) of the cohesive soil samples. If Neill's curves were extrapolated to grain sizes characteristic of clays, one would expect cohesive soils to have a critical velocity that is less than 1 ft/sec. The chart reveals that the cohesive soils have critical velocities in the 3 to 6

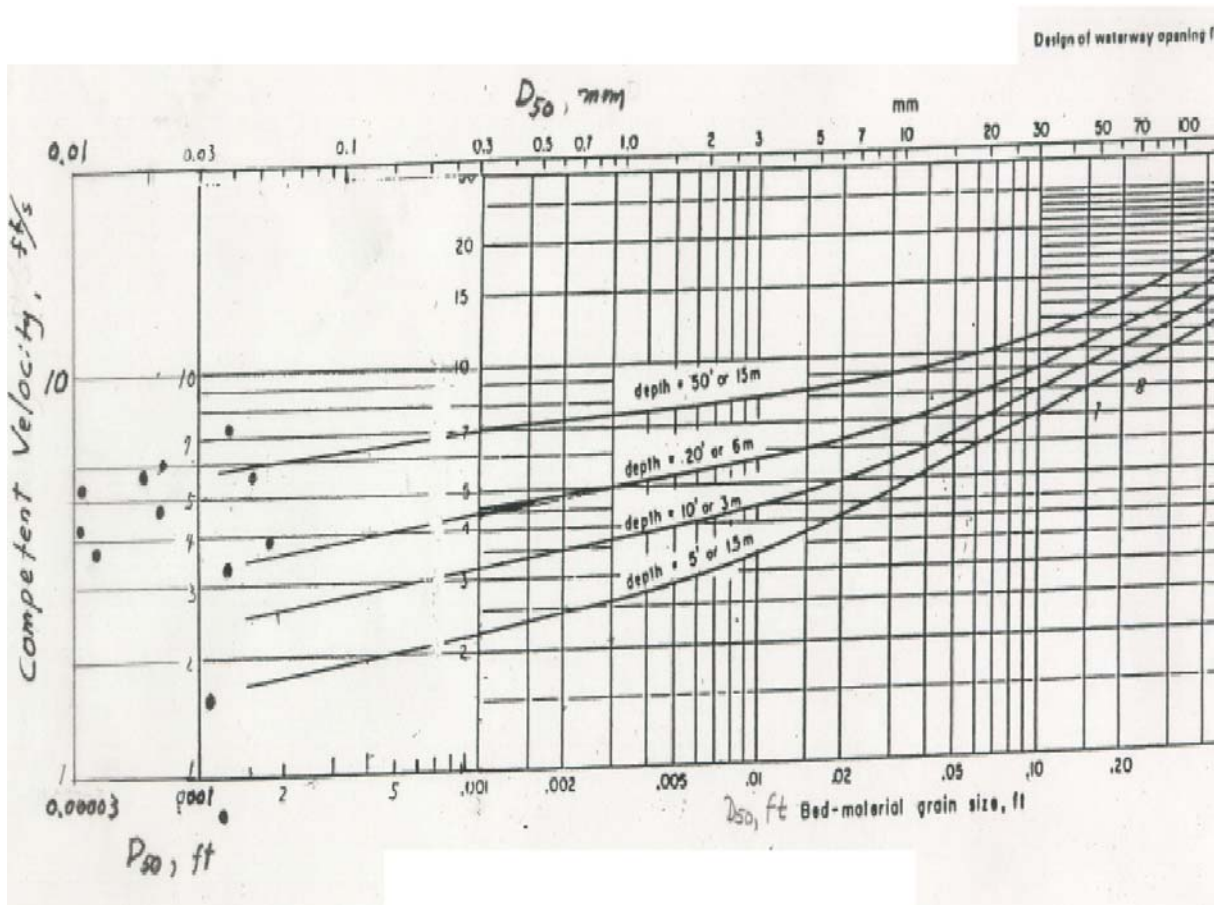


Figure 4.19. Neill's curves ("Suggested competent mean velocities for significant bed movement of cohesionless materials, in terms of grain size and depth of flow," showing extrapolation for finer particles (hand-drawn lines) and experimental results (dots).

ft/sec range. The source of Neill's data is unknown, but MSHA Office of Bridge Development personnel theorize that the Fortier–Scobey western canal velocity data are the basis of the curves. The Fortier–Scobey velocities were taken in open channels, whereas the critical velocity tests performed for this study were done in a closed conduit flowing full. Although the depth of flow (the height of the closed conduit) was only 2 inches, the samples were also subject to an unquantified pressure head produced by the water pump that may have contributed to the increased critical velocities in the EFA cohesive soils tests.

Because these clay soils do not have the same composition it is difficult if not impossible to make generalizations about the results. The experiment indicates, however, that if similar types of clay are tested over many samples, it may be possible to make equivalent Neill's Curves for cohesive soils for use as a reference for scour calculations. More

experiments of these cohesive soils were out of the scope of this study but it presents some interesting possibilities that could prove useful to cohesive scour computations in the future.

4.6. Use of Instantaneous Peak Discharges in Daily-Average Discharge Hydrograph

Briaud et al. (1999) recommend use of a daily discharge hydrograph for long-term scour prediction. The synthetic streamflow method developed in this study is designed to capture the statistics of daily discharge for an ungaged watershed. The 100-yr (Q100) discharge estimated by GISHydro2000 and used in MSHA design procedures is an instantaneous annual peak flow, which has a different statistical distribution. Peak flows generally last for a short time, and the corresponding daily average flow could be considerably smaller. Therefore, one would not expect that the 99th-percentile simulated daily-average discharge to be as large as the instantaneous Q100. However, since current MSHA design procedure dictates the use of instantaneous peak flows, the instantaneous Q100 was inserted into the daily-flow hydrographs using the SRICOS option and was treated as if it lasted for 24 hours. The question was raised, what is the effect on scour if the instantaneous peak discharge is assumed to last for 24 hours, rather than a more realistic duration? This section describes an exercise to investigate the effects of this assumption on scour due to an event that includes the 500-year instantaneous peak.

SRICOS allows short-term event simulation using a shorter time step. Starting from the estimated instantaneous Q500, several different event hydrograph models were developed. (It should be noted that there is no generally accepted method to simulate an event hydrograph, given a peak flow.) Standard design methods, such as SCS, assume a triangular hydrograph. Dillow (1998) suggests a standard event hydrograph whose parameters can be calculated from regression equations. Eight different event hydrographs were constructed, each having as its peak the 500-year instantaneous discharge for MD 26 over the Monocacy River. The hydrograph ordinates were specified every 15 minutes. These event hydrographs were run through the SRICOS program and the total event scour was analyzed. This scour was compared to the predicted scour that would result from a variety of averaging assumptions as described in Table 4.4.

The maximum scour depths are dependent on the assumptions that form the basis of

Table 4.4. Hydrograph Assumptions Used in the 15-Minute Discharge Experiment

Index	Name	Explanation	SRICOS Event Scour (ft)
A	Dillow	As recommended in Dillow (1998)	7.82
B	Dillow Event Peak, Event Duration	The peak discharge from A is assumed to apply for the duration of the entire event (55.75 hrs)	N/A
C	Dillow Event Mean, Event Duration	The event average from A is assumed to apply for the duration of the entire event (55.75 hrs)	7.82
D	Dillow 24-hr Peaks, 24 Hr Each	The event in Hydrograph A is split into 24-hr periods, and the peak flow within each 24-hr period is assumed to apply for that period	7.82
E	Dillow 24-hr. Means, 24-hr Each	The event in Hydrograph A is split into 24-hour periods, and the average flow over each 24-hour period is assumed to apply for that period (This is what the daily Q record would show if this event actually occurred, starting at midnight)	7.95
F	SCS Event	Triangular	7.95
G	SCS Event Mean, Event Duration	The event average is assumed to apply for the duration of the entire event (56.25 hr)	8.2
H	Peak 24 Hr	The peak discharge is assumed to apply for 24 hours (This is what we get when the Q peak is "inserted" into the hydrograph for SRICOS)	8.42

the hydrograph model. Hydrograph B, which assumed the peak discharge lasted the entire duration of the Dillow hydrograph (55.75 hr) could not be run, due to an unexplained error in SRICOS. The 24-hour peak discharge, Hydrograph H, produced the largest scour depths, a 7.7 percent overestimate with respect to the Dillow (1998) event hydrograph (A), and 5.9 percent over estimate with respect to the SCS event hydrograph (F). Hydrograph H does not represent a typical storm event, but it does indicate that using an estimated peak flow over a 24-hour duration in SRICOS tends to overestimate event scour, and possibly long-term scour as well. This overestimation would be greater for smaller watersheds, where flood flows are “flashy” and of short duration, and less significant for larger watersheds, where flood flows are attenuated and longer-lasting.

It is not the intent of this experiment to determine the best assumptions to be used in modeling hydrographs for scour studies, but rather to show how assumptions can affect the predicted maximum scour depths. It is recommended that more study and research be implemented in the future to determine the best hydrograph time scale and/or event model to use for scour prediction.

4.7. Discharge Order

This study devoted substantial effort to a method to create realistic discharge hydrographs. The synthetic hydrograph method attempts to capture seasonal variations in the average and range, as well as day-to-day persistence, of streamflow. Briaud et al. (2002) took a different approach to “future hydrographs,” using probabilistic methods to sample values from a statistical distribution whose mean and standard deviation do not change throughout the year, and assuming that each day’s discharge is independent of the previous day’s. In examining the results, the question was raised: how important is the order of discharges in the SRICOS scour calculation? The following investigation was conducted to explore that question. A “big flood”(100-yr) and “little flood” (10-yr) were selected from the peak flow estimates for MD 26 over the Monocacy River. The SRICOS equations were solved manually for a simple hydrograph consisting of two 24-hour discharges: First, the “big flood” followed by the “little flood,” then with the order reversed. SRICOS predicted scour of 7.6 ft for both two-flow sequences. In the “big-flood/little-flood” case, the big flood scoured 7.4 ft and the little flood added 0.2 ft of scour; in the “little flood/big flood” case, the little flood scoured 5.6 ft, and the big flood added 1.8 ft of scour. Operating on the 160-year sequence of flows, SRICOS predicted 7.74 ft of scour, with the majority of that scour occurring due to a single event (Fig. 4.15). In conclusion, although smaller storms do cause some scour, it is a minimal amount compared to the contribution of large storms, which account for the maximum value of scour, regardless of the order in which these flows occur.

5. Discussion

The Erosion Function Apparatus (EFA) and Scour Rate in Cohesive Soils (SRICOS) program were evaluated as a package in this study. Although related, the two technologies are actually separable and somewhat independent. Section 5.1 comments on the investigators' experience with the EFA, and Section 5.2 discusses the SRICOS software.

5.1. EFA Erosion Modeling

Soil in a riverbed acts a porous, semi-rigid boundary. The soil particles resist horizontal movement due to shear stress of water flowing over them, and resist vertical movement that arises from water pressures building up in pores within the soil bed, below the particles. The principle resistance to movement in cohesionless soil is by particle self-weight and by interlocking between adjacent particles in the soil bed. In the case of cohesive soils, other physical factors come into play that bind particles into larger units which usually results in greater resistance to erosion. Details of those units, including frequency and orientation of cracks, and mineralogy of the soil, both in situ as well as the representativeness of soil in the Shelby tube samples, will be important in characterizing erodibility of soil. Physical tests of erosion are certainly warranted, and the EFA is a step toward developing such a test. The following comments are made in the spirit of issues to consider in improvement of the EFA.

The EFA/SRICOS method predicts erosion of soils in riverbeds, assuming that flow is parallel to the soil surface. Once scour begins, however, the flow near the bottom of a scour hole moves in both vertical and horizontal directions, rather than in the straight flow seen in the EFA flume. This flow condition leads to more aggressive erosion behavior, because the dynamic pressure is greater and the pore pressure within the voids below the particles is increased. The particles move upward into the stream bed when the pore pressure is greater than the weight of the particles. Vertical components of velocity are found at the bottom of a pier and it is likely that this velocity is key to particle movement in pier scour holes. The EFA flow conditions are, arguably, unconservative because it applies flow parallel to the soil surface and does not account for vertical components of erosive flow.

Improvement in this regard is recommended.

In its implementation, the EFA presented some difficulties in obtaining satisfactory erosion rates. First, the proscribed method of pushing the sample 1mm into the streamflow introduces eddies around the sample that may cause scouring that is not caused by only the flow velocity.

Another difficulty is related to the difficulty of keeping 1mm of the sample in the streamflow. Not only is this difficult to assess, the fact that scour was rarely even across the sample surface meant that the decision of when to advance the soil became problematic. In one case, for example, a portion of a sample eroded more than 10mm on one side while another portion of the same sample remained unaffected by erosion. This led to uneven flow regardless of whether the soil was advanced.

The time to advance the soil also became a concern when testing at high velocities. The computer controlled push of the EFA piston led to a lag time of 1-2 seconds before the push occurred. At slow velocities this was not a matter of concern, however at higher velocities this lag produced erosion rates that were slower than what was actually seen. These slower rates then underestimate the amount of scour for a given velocity on the hydrograph.

After erosion commenced, the opacity of the water became an issue. The dirty water that quickly developed made observation of the sample difficult. The use of filters and possibly an automated method of determining when to push the sample could prove useful and improve repeatability.

Finally, characterizing erosion by conducting an erosion test on a real soil sample that includes natural layering and other non-uniformities, will be flawed because soil at different depths in the sample is likely to have different resistance to erosion.

The SHA OMT identified several issues in adjusting the velocity in the EFA. The test requires that the velocity be adjusted to the desired value (0.3 m/s, 0.6 m/s, etc.) within 30 seconds. This is supposed to ensure minimum distortion to the sample, before readings can be taken. With the current EFA system, it takes a much longer time (1 minute or more) to set the desired flow velocity. It was found that the velocity reading fluctuates within a certain range even if the desired flow is set. For example, if we set the velocity to 0.6 m/s, it is found to vary between the ranges of 0.54 m/s to 0.65 m/s. Sometimes the fluctuations are even

higher. In addition, there is a lag of a few seconds between an operation on the flow adjuster knob and the reading displayed on the monitor.

The EFA manual suggests that the operator must determine by visual inspection the point at which 1 mm of scour has occurred. Samples tested in the EFA at MSHA exhibited undulations on the scour surface that did not have a uniform depth. For example, more scour was observed on the sides of the tube walls than at the center of the sample (Fig. 5.1). The sample tends to be removed in chunks, causing undulations as deep as 2mm or more (Fig. 5.1). The uniformity and reproducibility of results across multiple observers is a concern. Briaud et al. (1999) report a comparison among observers; they found that multiple observers made very similar observations of scour for Texas soils. That study is not necessarily

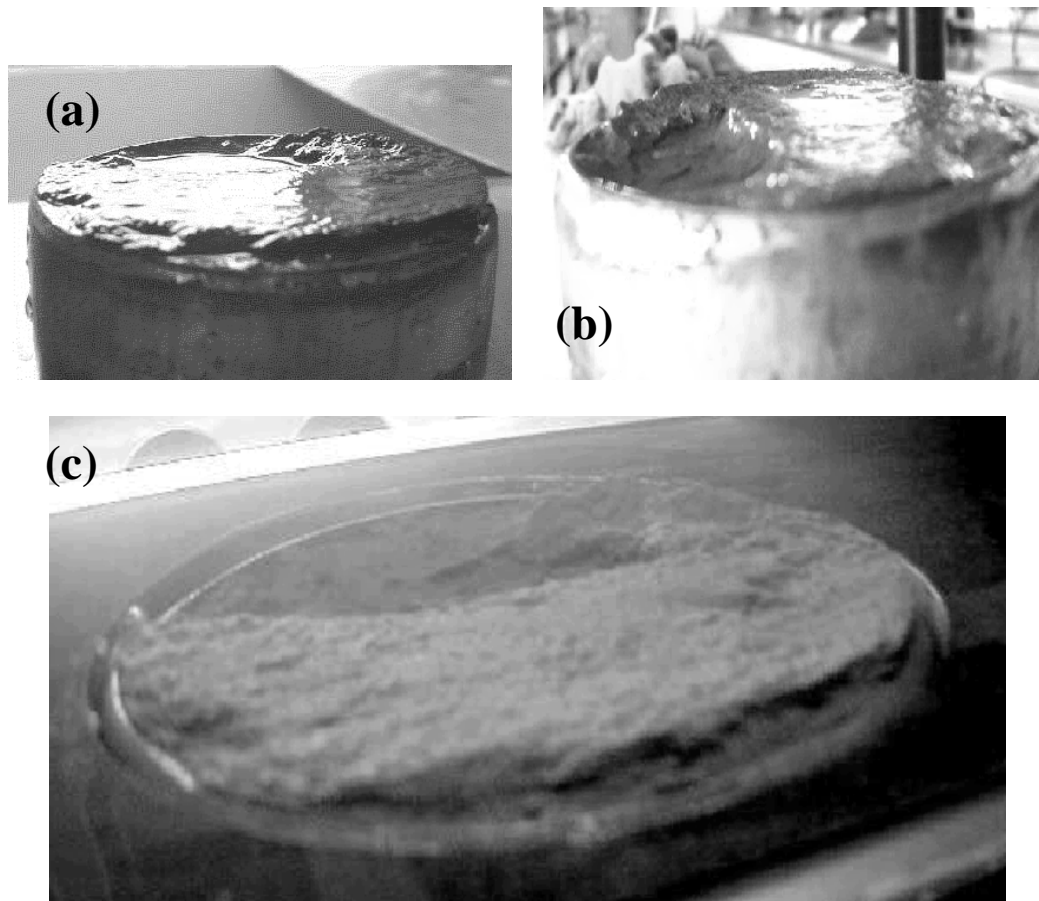


Figure 5.1. Soil samples undergoing EFA testing, showing greater scour at the tube walls than at the center and undulations deeper than 2 mm due to the removal of soil in chunks rather than by particles. All the Shelby tubes shown have outside diameter 76.2 mm. (Photos by MSHA)

applicable to Maryland soils.

A possible solution to the issue of dependence on visual interpretation would be a sensor capable of determining the micro-topography of the entire sample surface. Such a device could automatically compute the areally averaged scour depth, and reduce observer subjectivity.

5.2. SRICOS Modeling

There are two components of the SRICOS scour prediction program. First the soil characteristics of layer thickness and the shear stress at the proscribed EFA velocities and second the stream hydrograph with a user determined length. Both of these components pose some challenges.

The EFA erosion rates and computed shear stress from the experimental results are the foundation of the SRICOS scour analysis. As noted above in 5.1. the erosion rates may be underestimated due to the lag time involved in pushing the sample soil. In addition these erosion rates do not account for the vertical components of velocity that occur at piers. The predicted scour depths reflect the inadequacies of the experimental method.

Whether using the standard USGS stream hydrographs or generating synthetic hydrographs, there is still debate about what are the best hydrographs for the intended purpose (as noted in Section 4.6). Using the average daily flow as the basis for the hydrograph is not conducive to capturing the high peak flows of large storm events. These high flood flows do most of the scouring at a structure, but generally last only a few hours in even the largest watershed. By using the average daily flow, these peak flows are averaged out and the effects from these peak flows are missed in the scour computations. Inserting an instantaneous peak flow into the daily flow hydrograph is likely to overestimate scour because the peak flow is assumed to last 24 hours.

The synthetic hydrograph technique creates a sample from a realistic statistical distribution of daily discharge. This means that for any given day, a base flow or a slightly larger flow is more likely to be generated by the program than a large flood event. Therefore even when large numbers of hydrographs are generated, it is likely that no large discharges may appear. The result is hydrographs that may be underestimating maximum scour depths.

It is hoped that the hydrograph synthesis model developed in this study will be useful in producing random realizations of future streamflow that reflect appropriate return period characteristics and values of extreme flows. The regression equations developed in this study to estimate parameters of a hydrograph synthesis model indicate that the model parameters are driven by physical characteristics expected to change in the course of watershed development, including urbanization, imperviousness, and forest cover.

5.3. SRICOS Estimates of Scour Compared to HEC-18

As expected, the ultimate scour predictions by EFA-SRICOS were generally lower than those predicted by the HEC-18. The EFA-SRICOS provides a method to account for cohesive soils' greater resistance to erosion, while the HEC-18 equation assumes that the soil behaves like a sand. It is difficult to compare the two methods strictly, however, given the differences in their approach and hydrologic/hydraulic input requirements.

6. CONCLUSIONS

The conclusions of this study are framed in the context of the research hypotheses presented in Chapter 1. Sections 6.1 through 6.3 summarize conclusions relevant to each research hypothesis. These sections are followed by sections on limitations of current approaches to predicting bridge pier scour, and of EFA and SRICOS in their present state of development (EFA is a physical test that is separable from the SRICOS computational tool; therefore the two should be assessed separately, even though they are proposed as a package). Finally, this chapter closes with recommendations for future research.

6.1 Characterizing Maryland Soils with EFA

Hypothesis (a): The use of the Erosion Function Apparatus would allow characterization of the erodibility of cohesive soils at bridge crossing sites in Maryland.

The EFA was successfully used to obtain data on shear stress vs. erosion rate for several samples of Maryland soils. The geographic range within which appropriate soils are found in Maryland is fairly narrow, largely limited to the Piedmont province. The spatial variability of the soils in this province lends some doubt as to whether one or several Shelby tube borings actually capture the erodibility characteristics of the soils in which bridge piers are constructed. In addition, Maryland soils are geologically quite complex; the presence of small rocks and pebbles in clay presented challenges for sample collection and EFA analysis.

The EFA results are imperfect estimates of erosion rates in cohesive soils. They do not account for the vertical components of velocity at a pier and, as a result, may underestimate scour rate. The natural layering and non-uniformity of the soil can lead to under or over estimation of the rate of erosion. The mechanical difficulties of pushing the sample into the streamflow caused delays that can also result in underestimation of scour rate. However, the EFA does provide a method of determining erosion rates from actual soil samples that was not possible before.

6.2. Method to Create Synthetic Hydrographs for Ungaged Sites in Maryland

Hypothesis (b): The statistical analysis of gaged streamflow would reflect the effects of measurable watershed characteristics on magnitude, timing, and persistence of high flow events (scour-causing events) and allow the synthesis of realistic long time series of discharge for ungaged watersheds.

A method has been developed to create synthetic daily discharge hydrographs of any duration for ungaged sites in the Piedmont and Coastal Plain provinces of Maryland. This method is based on analysis of all gaged stations with at least 30 years of record. Parameters of the synthetic hydrograph model are estimated using prediction equations based on physical parameters that can be obtained automatically using the State of Maryland's Geographic Information System, GISHydro2000. The method successfully captures interannual and seasonal variability and autocorrelation in discharge. It produces time series of annual peaks that are consistent with existing conditions or conditions of the past several decades; however, the regression equations are based on past and current conditions, and further development is required in order to make predictions for future, changed conditions (such as ultimate development).

6.3. Reduction of Predicted Scour Depth with SRICOS

Hypothesis (c): Using the same hydrologic/hydraulic inputs, the EFA/SRICOS method would predict less scour than current methods that are based on non-cohesive soils.

When the HEC-18 predicted scour depths were compared to the SRICOS predicted scour depths, SRICOS does show a significant reduction in predicted scour depths in four of the five sites as seen in Table 4.3, even with a hydrograph of 160 years duration. However, given the conservative MSHA policy of estimating at least 5 feet of scour at a pier, the predicted scour depths at three of the sites would be raised to the minimum 5 feet of scour. The SRICOS method may be better suited to bridge piers in the channel as opposed to the overbanks as studied here.

The notion of a time dependent scour prediction model is enormously intriguing. The EFA/ SRICOS method may be used for the time being as another factor to consider in scour

prediction, but not the sole basis of the scour prediction. It is appropriate and understandable that designs that lead to less conservative assumptions of scour depth will require verification of those predictive methods, including field results if feasible. Verification of currently used methods is limited and tentatively suggests that HEC-18 scour predictions are conservative. If the mechanical difficulties of using the EFA can be overcome, if reasonable hydrograph assumptions can be determined, and if soil characteristics can be incorporated into the method, then the EFA and possibly SRICOS may have the potential of becoming an accepted design scour prediction.

6.4. Limitations of Current Approaches to Bridge Pier Scour in Cohesive Soils

The major limitation of current approaches is the application to cohesive soils of methods developed for, and tested with, non-cohesive soils (sand, gravel, cobbles). As discussed in this report and elsewhere, cohesive soils resist erosion through different physical mechanisms than non-cohesive soils. In addition, when subjected to erosion, cohesive soils exhibit different behavior, in particular, removal in clumps rather than particle-by-particle. Thus the assumptions in current methods concerning scour rate and scour hole geometry are not properly applied to cohesive soils.

6.5. Limitations of the EFA

The EFA was designed to address the problem discussed in Section 6.4: it quantifies physical scour on real soils. It is an emerging technology, and is evaluated as such in this report and these comments; indeed, MSHA's role in undertaking this study was to participate in evaluating and improving the method.

Challenges in applying the EFA to determine the erosion rate for soil samples included equipment issues, operator issues and sampling issues. These issues are discussed in Chapter 5 of this report. In the course of this study, a calibration problem was identified and corrected. Concerns arose about the correct interpretation of shear stress in the testing flume. The reliance on the visual judgment of the operator lends a certain non-reproducibility to the analysis. Visibility is impaired at high flow rates, due to the entrainment of eroded sediment

in the flume flow; as a result, it is even more challenging for the operator to judge the rate of erosion under physical conditions that are most critical for scour prediction.

Whereas cohesionless soils may erode particle by particle, cohesive soils have complicating attributes. For example, fissures in clay may create vulnerability for erosion of clumps of cohesive soil and the sample may or may not capture representative fissuring. The geometry of developing scour holes and the resulting fluid forces introduce complex physical behavior (including 3-dimensional eddies and pressure effects) that cannot be captured in the EFA, which is designed to quantify tangential shear stress. Indeed, the physical scale dictated by laboratory testing of soil properties may preclude ever being able to capture such field-scale phenomena. In addition, Maryland soils exhibit great variability in their physical properties, both laterally and vertically. Although the EFA is a real physical test of real soil, the fact that specimens are not uniform indicates a need to develop protocols for sample collection (how many, where) and use of multiple cores' data in the subsequent analysis (For example, the differences among the three cores for MD 7 at Whitemarsh).

6.6 Limitations of SRICOS

The ability to predict the long-term evolution of bridge pier scour is a novel attribute of the SRICOS method. Historic or simulated hydrographs may or may not include the extreme events that contribute the majority of scour, raising concerns about whether a particular simulation actually captures the scour-generating discharges of concern to designers. Although SRICOS allows the user to insert the 100- and 500-year flood events into the hydrograph, there is an incongruity in inserting instantaneous peak flows into a hydrograph of daily discharges. Daily discharge hydrographs are appropriate for predicting the long-term evolution of scour; in such cases, the events associated with the peak discharges should be disaggregated or averaged to daily flows. For design calculations, where rare extreme events must be considered, event hydrographs on a shorter time step may prove more appropriate.

Current MSHA bridge design practice requires that piers be designed for ultimate scour, regardless of the probability that such an event will happen in the lifetime of the bridge. A long-term simulation using SRICOS is not necessary to address this question.

Applying SRICOS to a single, extreme event (as explored in Section 5.6) may be more consistent with MSHA design philosophy; however, the SRICOS method does not currently provide guidance for constructing a realistic event hydrograph based on estimated peak discharge.

Finally, SRICOS ultimate scour predictions do not appear particularly sensitive to physical realism in the hydrologic time series; randomly-ordered discharges give the same results as physically-realistic persistence in flows. This raises some concern about the physical realism of the method: it would seem that the order and duration of discharge events should affect not only the evolution of scour in time, but perhaps also the ultimate scour depth. Physical reasoning would seem to indicate that the sequence of high flows, and the re-filling of scour holes between extreme events would affect the timing and magnitude of ultimate scour. However, the SRICOS method computes ultimate scour as a sequential addition of contributions by daily flow, and does not explicitly model between-flood periods.

6.7. Limitations of New Synthetic Hydrograph Technique

Because the hydrograph synthesis equations were based on current and historic conditions, the hydrographs produced may not accurately reflect future (i.e., ultimate development) extreme events. More sophisticated techniques of statistical and physical hydrology will be required to calibrate and apply the model over changing conditions.

Additionally, as discussed in Sections 5.2 and 6.6, any single probabilistically-generated synthetic hydrograph may or may not include the extreme events whose analysis is dictated by life safety concerns. If design philosophy specifies a particular magnitude or frequency of event, then a deterministic simulated hydrograph is a better choice. The new hydrograph technique may be most appropriate to risk-based implementations of SRICOS, as proposed in Briaud et al. (2002).

7. Recommendations For Future Research

The EFA and SRICOS represent emerging technologies, and this report is not intended to recommend their implementation as operational design tools at this time. This chapter presents some future research avenues suggested by this study and by the capabilities of the EFA/SRICOS approach.

We recommend that the MSHA continue to analyze soil samples from bridge pier sites using the EFA and make scour predictions using SRICOS. Collecting Shelby tubes at bridge sites is a standard part of site reconnaissance, and it would be convenient to collect several tubes for SRICOS analysis at the time the soil testing is done. SRICOS predictions can be made using the most appropriate hydrograph prediction tools at the time of each study; we would hope and expect that both the hydrologic prediction techniques and the SRICOS scour computation theory would advance as time goes on. Each site analyzed with SRICOS should be added to a long-term monitoring program as described below.

We recommend a long-term monitoring program for the study sites to determine the adequacy of the SRICOS predictions, and to contribute to ongoing improvements in scour prediction. The overbank piers in particular are amenable to a long-term monitoring program including measurement and photography of any scour holes that may develop, because they can be accessed and examined in dry weather without diving. SRICOS can be used to estimate probable ranges of scour after five years, ten years, etc.; investigators can then determine whether actual evolution of the scour holes falls within the predicted range. If the reduced scour depths predicted by EFA-SRICOS in cohesive soils can be demonstrated by long-term field observations, then future bridge piers might be designed to be most cost-effective than those based on conservative, non-cohesive soil assumptions.

There are specialized design and analysis problems where the use of EFA could be helpful in decision making, for example, evaluation of scour critical bridges, bridges with a limited remaining service life, or bridges with unknown foundations. We recommend that MSHA continue to explore such applications of this innovative instrument.

Linking soil properties and hydraulic data, and the ability to predict the time evolution of bridge pier scour are novel and valuable attributes of the SRICOS method. The probabilistic, risk-oriented approach demonstrated in Briaud et al. (2002) is a promising

contribution to the field, and it is hoped that these avenues will be pursued. The Monte Carlo approach could be applied to uncertainty in the Erosion Function inputs as well as to variability/uncertainty in future hydrographs.

Risk-oriented approaches are not yet widely accepted for bridge design. Life safety concerns dictate that bridge piers must be designed to withstand the worst-case scour-causing discharge. If MSHA chooses to apply SRICOS as a design tool, the issue of mixing instantaneous discharge estimates with a daily-average hydrograph must be addressed. As shown in the research results, the single, inserted extreme values contribute most or all of the scour, and the effort to create a realistic long-term probabilistic simulation is unnecessary. Using SRICOS on a single-event basis shows promise for comparability with HEC-18; however, this requires rigorous methods to construct realistic event hydrographs from estimated peak flows.

Whether predicting a single ultimate value or the time evolution of erosion, scour prediction methods for bridge design require estimates of future flows. Methods to estimate extreme discharges under changed conditions are a topic of great interest and discussion in the field of hydrology, and there is a great deal of uncertainty in estimates of, for example, future 100-year and 500-year discharges, even in gaged basins. Ongoing work by G. Moglen and colleagues, in collaboration with MSHA and USGS, is exploring improvements; their work should be incorporated into further developments of the hydrologic synthesis aspects of the present study.

With growing interest in the temporal evolution of scour, the specification of realistic discharge and velocity hydrographs is critical to the SRICOS method. More sophisticated techniques of statistical and physical hydrology will be required to calibrate and apply the Synthetic Hydrograph model under changing conditions.

This study invested considerable effort in developing a method to capture the correct timing (rise and fall) of flood hydrographs, as well as peak flow statistics. It was disappointing to find that the SRICOS predictions were relatively insensitive to physical realism in the hydrograph, and that the statistical approach may not address the needs of MSHA bridge design philosophy; nonetheless, we hope that this method will prove useful for hydrologic applications in Maryland.

8. References

- Abdel-Rahmann, N.M., 1964. "The Effect of Flowing Water on Cohesive Beds," Contribution No. 56, Versuchsanstalt für Wasserbau und Erdbau an der Eidgenössischen Technischen Hochschule, Zurich, Switzerland, pp. 1-114.
- American Society of Civil Engineers (ASCE), 1977. "Sedimentation Engineering," Manual No. 54.1977.
- Annandale, G.W., 1999 "Scour of Rock and Other Earth Materials at Bridge Pier Foundations". Golder Associates Inc., 44 Union Blvd, Suite 300, Lakewood, Colorado 80228.
- Ansari, Kothyari, and Rangaraju, 2002. "Influence of Cohesion on Scour around Bridge Piers," *Journal of Hydraulic Research*, Vol. 40, No. 1, pp. 717-719.
- Briaud, J.-L., F. Ting, H.C. Chen, R. Gudavalli, B.P. Kwak, S.W. Han, S. Perugu, G. Wei, P. Nurtjahyo, Y. Cao, and Y. Li, 1999. "SRICOS: Prediction of Scour Rate at Bridge Piers". Report 2937-1, Texas Department of Transportation, December 1999.
- Briaud, J.L., F.C.K. Ting, H.C. Chen, S.W. Han, and K.W. Kwak, 2001a. "Erosion Function Apparatus for Scour Rate Predictions," *Journal of Geotechnical and Geoenvironmental Engineering*, pp. 105-113.
- Briaud, J.-L., H.C. Chen, K.W. Kwak, S.W. S.W. Han, and F.C.K. Ting, 2001b. "Multiflood and Multilayer Method for Scour Rate Prediction at Bridge Piers," *Journal of Geotechnical and Geoenvironmental Engineering*. pp. 114-125.
- Briaud, J.-L., P. D'Odorico, and E.J. Jeon, 2002, "Future Hydrographs and Scour Risk Analysis," Proceedings of the First International Conference on Scour of Foundations, Vol. 1, pp.272-282, Texas A&M University, College Station, Texas, USA
- Briaud, J.-L., H.-C. Chen, Y. Li, P. Nurtjahyo, and J.Wang, 2003. "Complex Pier Scour and Contraction Scour in Cohesive Soils." NCHRP Report 24-15.
- Dunn, I.S., 1959. "Tractive Resistance of Cohesive Channels," *Journal of the Soil Mechanics and Foundations Division, ASCE*, No, SM3, Proc. Paper 2062, pp. 1-24.

- Einstein, H.A., and E.S.A. El-Samni, 1949. "Hydrodynamic Forces on a Rough Wall," *Review of Modern Physics*, Vol. 21, pp.520-524.
- Federal Highway Administration (FHWA), 2001. HEC-18, National Highway Institute Evaluating Scour at Bridges, 4th edition, Publication No. FHWA NHI 01-001.
- Henderson, F.M. 1996. *Open Channel Flow*, Prentice-Hall, Inc., Upper Saddle River, New Jersey.
- Flaxman, E.M.. 1963. "Channel Stability in Undisturbed Cohesive Soils," *Journal of the Hydraulics Division, ASCE*, pp 87-96.
- Grissinger, E.H., 1966. "Resistance of Selected Clay Systems to Erosion by Water," *Water Resources Research*, Vol. 2, No. 1 pp. 131-138.
- Grissinger, E.H. and L.E. Asmussen, 1963. Discussion of "Channel Stability in Undisturbed Cohesive Soils," *Journal of Hydraulics Division*, pp. 259-261,
- Guyen, O., J.G. Melville, and J.E. Curry, 2003. "Analysis of Clear Water Scour at Bridge Contractions in Cohesive Soils," *Transportation Research Record*, 1797, Paper No. 02-2127.
- Hanson, G.J., and A. Simon, 2002. Discussion of "Erosion Function Apparatus for Scour Rate Predictions." *Journal of Geotechnical and Geoenvironmental Engineering*, pp. 627-628.
- Kamphuis, J.W., 1990. "Influence of Sand or Gravel on the Erosion of Cohesive Sediment," *Journal of Hydraulic Research*, Vol. 28, No. 1, pp. 43-53.
- Kuti, E.O., 1976. "Scouring of Cohesive Soils". *Journal of Hydraulic Research*, Volume 14, No. 3.
- Leopold, L., 1994. *A View of the River*. Harvard University Press, Cambridge.
- Melville, B.W. and Y.-M. Chiew, 1999. "Time Scale for Local Scour at Bridge Piers," *Journal of Hydraulic Engineering*, pp. 59-65.
- Moglen, G.E., Casey, M.J., 2000 "GISHydro2000," University of Maryland for MSHA.

- Molinas, Abdeleayem, Abdou, Hosni, Noshi, and Reiad, 1996. "Summary of Effects of Gradation and Cohesion on Bridge Scour Vol. 4: Experimental Study of Scour Around Circular Piers in Cohesive Soils."
- Neill, C.R., 1973. *Guide to Bridge Hydraulics*. Roads & Transportation Association of Canada Univ. of Toronto Press, Toronto, Ontario, Canada. (Out of print, see TAC 2001, below).
- Salas, J.D., 1993. "Analysis and Modeling of Hydrologic Time Series," in *Handbook of Hydrology*, D. Maidment, ed., Chapter 19.
- Smerdon, E.T., and R.P. Beasley, 1961. "Critical Tractive Forces in Cohesive Soils," *Agricultural Engineering*, St. Joseph, Mich., pp.26-29.
- Transportation Association of Canada (TAC), 2001. *Guide to Bridge Hydraulics*, 2nd Ed., 2323 St. Laurent Blvd., Ottawa, Ontario, K1G 4J8 Canada.
- U.S. Army Corps of Engineers (USACE), 2002. *HEC-RAS, River Analysis System User's Manual*. U.S.A.C.E. Hydrologic Engineering Center (HEC) Report No. CPD-68, 420 pp.

APPENDIX A

Theory of Synthetic Hydrograph Technique

Following procedures described by Salas (1993), for each day of the year, the average and standard deviation of the $\ln Q$ across years are computed, as follows:

$$E[\ln Q(d)] = \frac{\sum_{\text{all years}} \ln Q(d, y)}{\text{number of years}} \quad (\text{A-1})$$

$$\text{StdDev}[\ln Q(d)] = \sqrt{E\{\ln Q(d, y) - E[\ln Q(d)]\}^2}$$

where

y = year

d = day, 1 to 366

$Q(y, d)$ = discharge [cfs]

$\ln Q(y, d)$ = natural logarithm of Q

$E[\ln Q(d)]$ = Daily expected value (mean) of $\ln Q$

$\text{StdDev}[\ln Q(d)]$ = Daily standard deviation of $\ln Q$

The $\ln Q$ data are further transformed by subtracting the corresponding interannual average value from each day and dividing by that day's interannual standard deviation. The result was a sequence of zero-mean, unit variance autocorrelated deviations (Z).

$$Z(y, d) = \frac{\ln Q(y, d) - E[\ln Q(d)]}{\text{StdDev}[\ln Q(d)]} \quad (\text{A-2})$$

The correlation of each day's Z value to the preceding day (across years) is computed, as follows:

$$\rho_z(d) = \sqrt{E[Z(d)Z(d-1)]} = \frac{\sum_{\text{all years}} Z(d, y)Z(d-1, y)}{\text{number of years}} \quad (\text{A-3})$$

This is a measure of persistence in flow; the analysis described here allows this persistence to vary seasonally, rather than assuming a year-round uniform value. (Many of the sites analyzed showed so little seasonal variation in this parameter that a constant value was applicable.)

A cosine-wave model was fit to the average $\ln Q$, the standard deviation of $\ln Q$, and the one-day correlation of Z . Each cosine-wave model has three parameters: mean, amplitude, and day of maximum. In the following models, A_i and B_i (dimension: natural log of discharge) are the mean and amplitude of the cosine wave, and τ_i (dimension: day) represents the day of the year at which the peak value occurs. B_i is always non-negative, and τ_i takes a value between 1 and 366.

$$\begin{aligned}
 E[\ln Q(d)] &= A_1 + B_1 \cos\left[\frac{2\pi}{366}(d - \tau_1)\right] \\
 \text{StdDev}[\ln Q(d)] &= A_2 + B_2 \cos\left[\frac{2\pi}{366}(d - \tau_2)\right] \\
 \rho_Z(d) &= A_3 + B_3 \cos\left[\frac{2\pi}{366}(d - \tau_3)\right]
 \end{aligned}
 \tag{A-4}$$

Given these parameters, synthetic streamflow hydrographs of any length can be generated as follows: A sequence of zero-mean, unit-variance, temporally-correlated deviations are generated using random sampling. A Pearson-3 (shifted gamma) distribution was found to be an appropriate distribution for standardized daily discharge (after removing the seasonal mean and standard deviation). Synthetic Z values are generated using, for example, the statistical function “Gamma Inverse” in Microsoft Excel, as follows:

$$Z(y, d) = \rho_Z(d)Z(y, d - 1) + \sqrt{(1 - \rho_Z^2)}\zeta(d)
 \tag{A-5}$$

where $\zeta(d)$ is randomly sampled from the zero-mean, unit variance Pearson 3 distribution. Each synthetic Z value is multiplied by the corresponding day’s standard deviation of $\ln Q$, added to that day’s mean of $\ln Q$, to give a time series of synthetic $\ln Q$. The $\ln Q$ values are

exponentiated to obtain the time series of Q . There is no limit to the length of the synthetic hydrograph that can be produced in this manner.

The steps of data analysis and hydrograph synthesis are demonstrated in Chapter 3 of this report using Whitemarsh Run at White Marsh, Md., as an example.

Figure 3.7(a) shows $\ln Q$ for the years 1959 to 2002 at White Marsh. A seasonal cycle in both mean and variance is clear from this figure: discharge tends to be both lower on average and more variable in the summer months. Figure 3.8 shows the resulting interannual mean and standard deviation for each day of the year at White Marsh, as estimated from the data record. The cosine-wave models derived for Whitemarsh Run are shown as the smooth curves in Figure 3.8. As observed in Figure 3.8, the mean $\ln Q$ reaches a maximum in early Spring (day 80), while the standard deviation of $\ln Q$ is highest in Summer (day 230). Figure 3.7(b) shows the data after mean and standard deviation of $\ln Q$ were removed (Z) for 1959 to 2002 at White Marsh. The correlation of Z on each day of the year to the preceding day (across years) is included in Figure 3.8.

Analysis of the Z data from White Marsh indicates that they are well represented by a Pearson 3 (shifted Gamma) distribution. Further, the deviations corresponding to days of the year appear to be drawn from the same distribution. Selected percentiles of the observed deviations (Z) were used to determine the parameters of the Pearson 3 distribution. Because the Z variable must have zero mean and unit variance, a single free parameter determines the shifted Gamma distribution: ξ , the distance of shift. This value was found by minimizing the maximum absolute difference between the sample and the computed percentiles (Kolmogorov statistic).

To transfer the properties reflected by the parameters of the cosine-wave models, multiple regression was used to determine a mathematical relationship between the parameters of the cosine wave models and physical characteristics of watershed that can be determined using automated tools in GIS-Hydro 2000, a Geographic Information System that has been developed specifically for use by MSHA in Hydrologic analysis. Different families of regression equations were developed for the Piedmont and Coastal Plain regions. Candidate predictor variables for the regression were the physical properties enumerated in the standard GIS-Hydro 2000 report for the watershed contributing to a selected point on a stream (typically, a bridge crossing site. Thus, there are 17 predictor variables proposed: (1)

Drainage Area (log transformed), (2) Channel Slope, (3) Land Slope, (4) Urban Area, (5) Impervious Area, (6) Time of Concentration [Hydrology Panel], (7) Time of Concentration [From SCS Lag Equation * 1.67], (8) Longest Flow Path, (9) Basin Relief, (10) Average Curve Number, (11) % Forest Cover, (12) % Storage, (13) % A Soils, (14) % B Soils, (15) % C Soils, (16) % D Soils, and (17) 2-Year, 24-hour Precipitation. An additional physical variable reported by GIS-Hydro 2000, % Limestone, was not used in this analysis because the study focused on the Piedmont and Coastal Plain regions, where karst formations (due to limestone) are not present and do not affect basin hydrology. Stepwise linear regression was used to identify the important predictor variables separately for each of the nine parameters off the cosine-curve synthetic hydrograph model. Final model selection was based on whether adding an additional variable improved the goodness of fit significantly (according to statistical measures) and did not introduce irrational regression coefficients.

Using the regional regression equations, the parameters of the synthetic hydrograph method can be determined for any bridge crossing location in either the Piedmont or the Coastal Plain. The method described above can then be used to generate synthetic hydrographs of any length for ungaged locations.

APPENDIX B

EFA Data Reductions

Tables of Erosion Rates, Velocity and Shear Stress from EFA tests of Sample Soils

MD 26, Tube 1, 4'-6'

vel(ft/s)	erosion (mm/hr)	shear (lbs/ft ²)
1.08	1.003	0.007
3.67	1.001	0.062
4.99	1.501	0.109
7.51	13.630	0.230
11.12	481.283	0.465

MD 26, Tube 2, 6'-8'

v (ft/s)	erosion (mm/hr)	shear (lbs/ft ²)
0.68	1.00	0.003
2.44	1.00	0.030
3.84	1.01	0.067
4.98	2.02	0.109
7.58	44.51	0.234
11.22	311.30	0.465

MD28, Tube B-3, 5'-7'

v (ft/s)	erosion (mm/hr)	shear (lbs/ft ²)
0.85	0.0	0.005
1.58	0.0	0.014
2.53	0.0	0.032
3.68	1.5	0.062
4.89	4.5	0.104
7.61	88.2	0.233
10.96	493.2	0.443

MD 28, Tube B-3A, 5'-7'

v (ft/s)	erosion (mm/hr)	shear (lbs/ft ²)
1.48	1.00	0.012
1.97	1.03	0.021
2.53	1.61	0.032
3.68	6.02	0.062
7.28	353.42	0.215
10.93	412.84	0.449

MD 28, Tube B-3, 7'-8.5'

v (ft/s)	erosion (mm/hr)	shear (lbs/ft ²)
0.76	1.000	0.004
1.57	1.000	0.001
2.49	1.000	0.003
3.68	8.004	0.062
5.12	1.003	0.113
7.48	4.043	0.218
10.96	135.135	0.438

MD 355, Tube 2'-4'

v (ft/s)	erosion (mm/hr)	shear (lbs/ft ²)
0.75	0.00	0.004
1.54	0.00	0.014
2.46	1.00	0.034
3.67	5.52	0.067
4.95	21.61	0.116
7.41	96.67	0.253
11.06	430.62	0.534

MD 355, 6.5'-8.5'

v (ft/s)	erosion (mm/hr)	shear (lbs/ft ²)
0.23	1.000	0.004
0.45	1.000	0.013
0.76	1.000	0.032
1.15	1.516	0.065
1.52	0.999	0.114
2.28	2.011	0.254
3.35	79.717	0.527

MD 7, Tube ,1 1'-3'

v (ft/s)	erosion (mm/hr)	shear (lbs/ft ²)
0.76	0	0.000
1.31	0	0.000
2.53	1.5	0.032
3.74	2	0.064
4.92	3.5	0.114
7.48	4.5	0.244
11.02	394.7	0.823

MD 7 Tube 2, 1'-3'

v (ft/s)	erosion (mm/hr)	shear (lbs/ft ²)
1.0	0	0.005
1.6	0	0.014
2.3	0	0.028
3.94	16.5	0.070
4.59	23	0.089
7.87	52.63	0.242
11.16	50	0.446

MD 7 Tube 3, 1'-3'

v (ft/s)	erosion (mm/hr)	shear (lbs/ft ²)
0.89	0	0.0
1.47	0	0.0
2.43	2	0.030
3.87	3	0.068
5.05	3.0	0.116
7.58	6.5	0.251
11.45	566.0	0.493

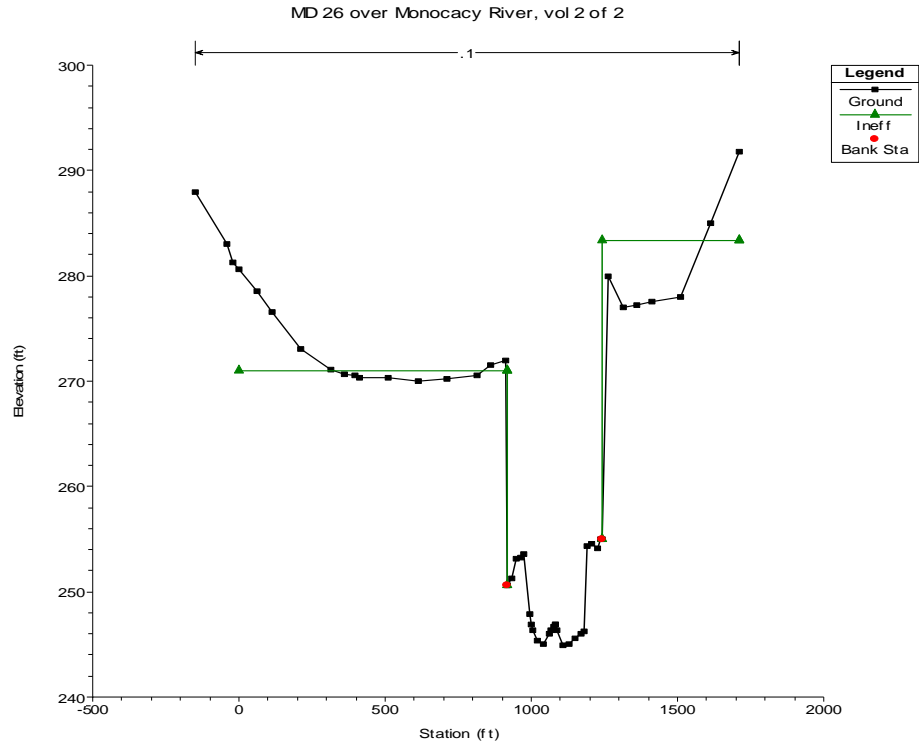
Woodrow Wilson 58'-60'

v (ft/s)	erosion (mm/hr)	shear (lbs/ft ²)
0.82	0	0.00
1.44	36	0.01
2.56	497	0.03
3.71	800	0.06

APPENDIX C

HEC-RAS Analysis

MD 26 over Monocacy River Upstream Bridge Cross Section

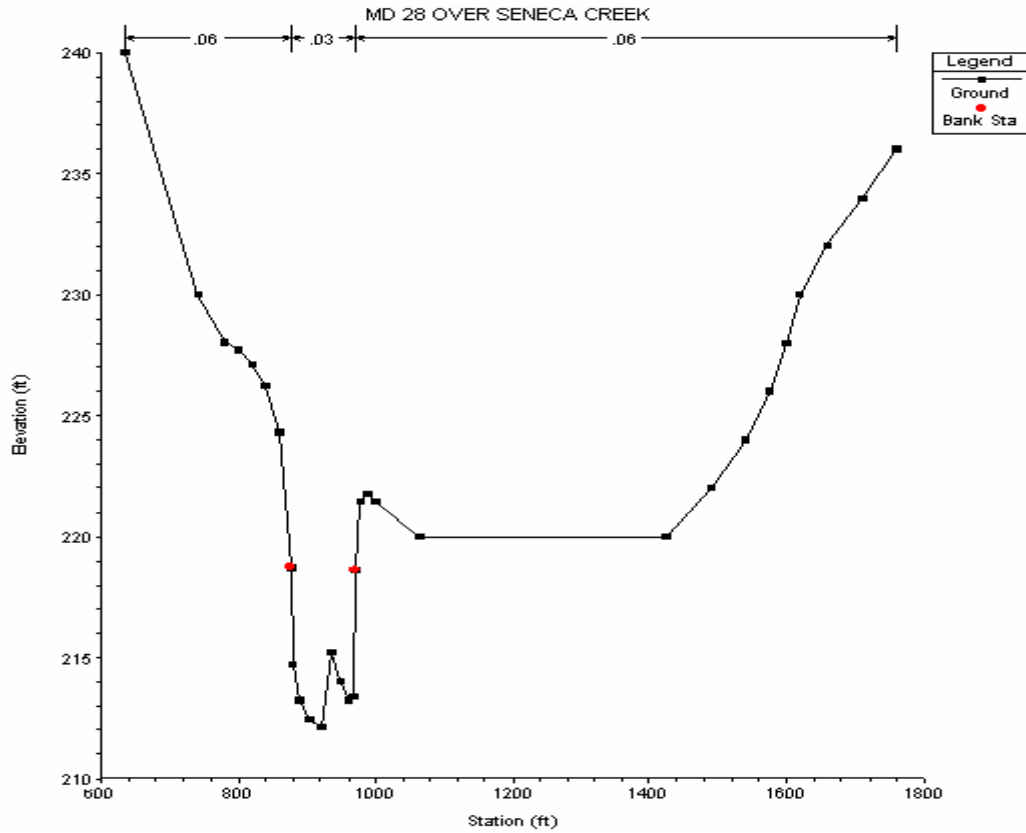


Velocity and water depth are computed by HEC-RAS at the location of the bridge pier, as if the pier were not there, following SRICOS procedure.

Reported velocity is between Stations 1053.4 and 1117.6

Q	Velocity (ft/s)	Water Depth (ft)
200	0	0
500	0.92	0.58
1000	1.52	1.72
5000	2.61	7.97
10000	3.02	12.98
19500	3.83	18.81
36600	5.49	23.89
67200	6.35	30.85
81600	6.46	33.57
138700	6.76	40.92

MD 28 over Seneca Creek Upstream Bridge Cross Section

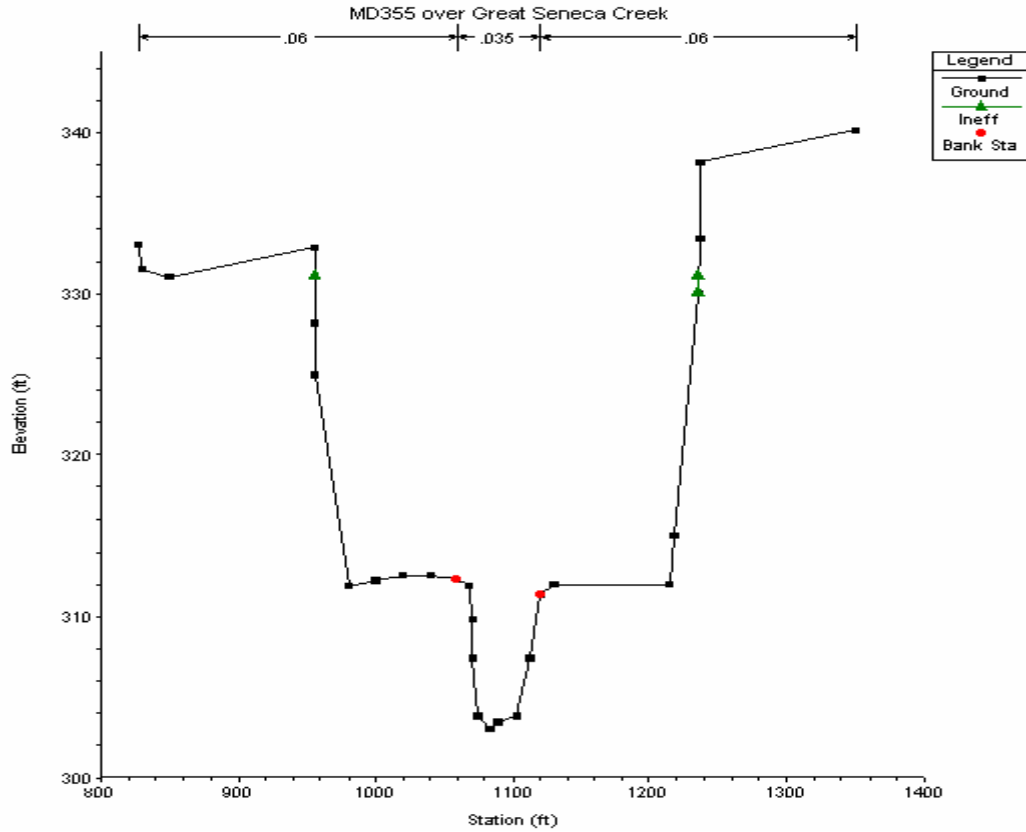


Velocity and water depth are computed by HEC-RAS at the location of the bridge pier, as if the pier were not there, following SRICOS procedure.

Reported velocity is computed between Stations 971 and 1128.8.

Q	Velocity (ft/s)	Water Depth (ft)
2950	0.04	0.02
5098	0.56	1
8960	1.19	2.73
9462	1.25	2.92
11600	1.49	3.67
14535	1.77	4.59
30470	2.48	10.07
51799	2.57	17.94

MD 355 over Great Seneca Creek Upstream Bridge Cross Section

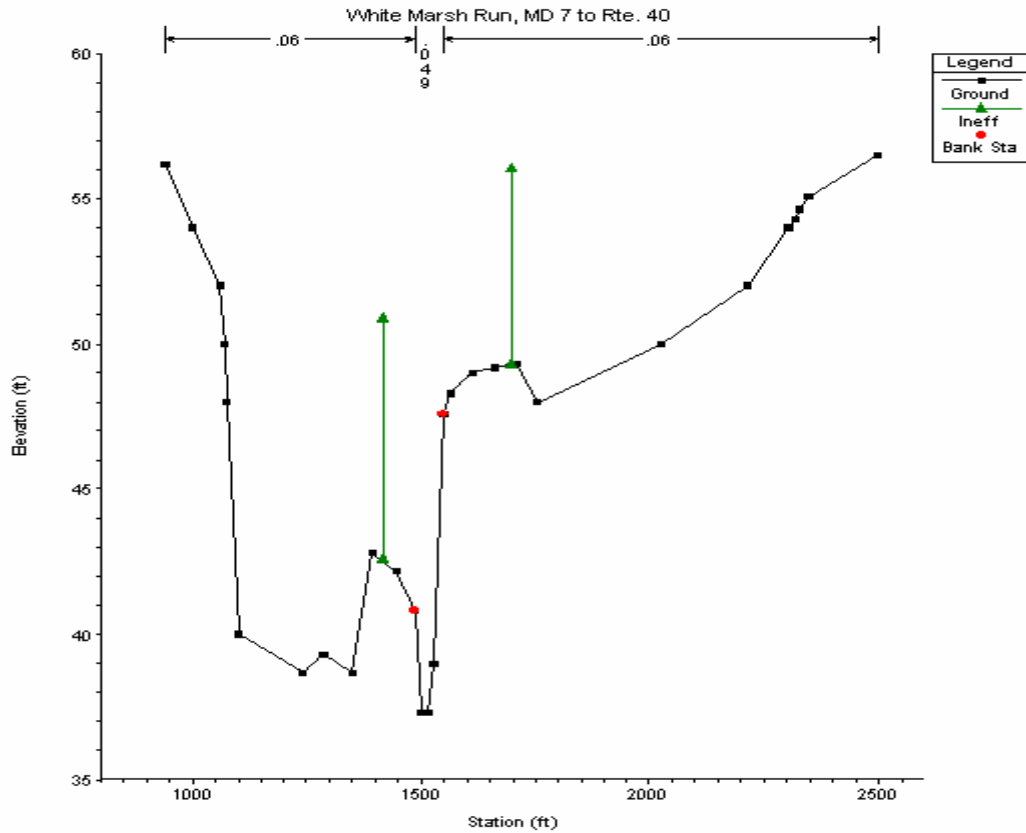


Velocity and water depth are computed by HEC-RAS at the location of the bridge pier, as if the pier were not there, following SRICOS procedure.

Reported velocity is computed between Stations 1037.7 and 1045.1

Q	Velocity (ft/s)	Water Depth (ft)
1000	0	0
1500	0.56	0.81
2000	1.13	2.06
3470	1.53	3.04
7600	2.56	6.31
10600	3.02	8.37
17400	3.65	12.73
29580	4.33	19.48

MD 7 over White Marsh Run Upstream Bridge Cross Section



Velocity and water depth are computed by HEC-RAS at the location of the bridge pier, as if the pier were not there, following SRICOS procedure.

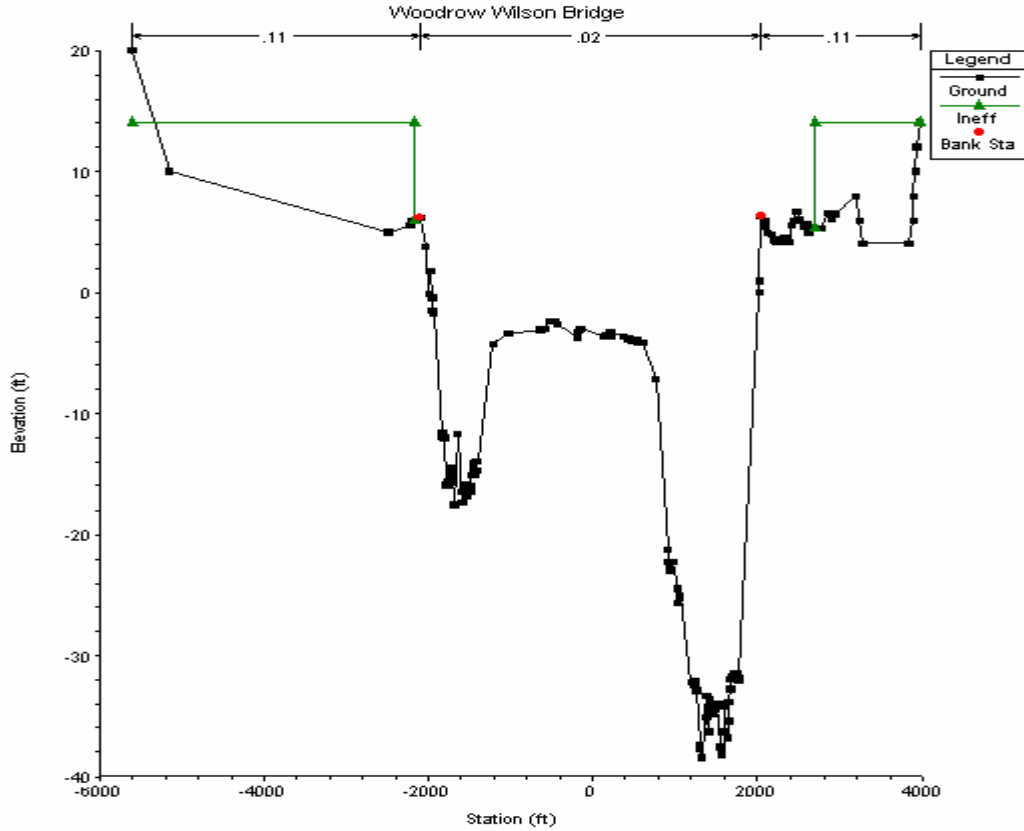
Reported velocity is computed between Stations 1473.4 and 1488

Q	Velocity (ft/s)	Water Depth (ft)
500	0.8	0.69
800	1.2	1.29
1880	2.6	4.37
4540	4.08	7.51
5300	3.99	7.44
6300	4.05	8.57
7500	1.07	11.69
8500	1.16	12.32
10700	1.36	13.48
12000	1.19	14.29

I-95 over Potomac River

Woodrow Wilson Bridge

Upstream Bridge Cross Section



Velocity and water depth are computed by HEC-RAS at the location of the bridge pier, as if the pier were not there, following SRICOS procedure.

Reported velocity is computed between Stations -1373.3 and -1269.9.

Q	Velocity (ft/s)	Water Depth (ft)
20000	0.22	11.95
120000	1.3	12.96
250000	2.6	14.39
330000	3.35	15.21
410000	4.1	15.74
480000	4.67	16.62
575000	5.42	17.68
700000	6.34	18.96